AN3183

Weight Scale Application using MCP3564 24-Bit Delta-Sigma ADC

Author: *Dana Diaconu,*
Microchip Technology Inc.

INTRODUCTION

This application note describes a weight scale design using Microchip's MCP3564 24-bit Delta-Sigma Analog-to-Digital Converter (ADC) and PIC24 microcontroller. The weight scale uses an automatic calibration process and techniques to minimize power consumption. The design takes advantage of the ADC's dynamic reconfigurability features of oversampling ratio (OSR) and Gain settings to demonstrate the impact of certain configurations on the precision and the accuracy of the device. These settings can be made from a dedicated graphical user interface (GUI) which also allows the calibration of the weight scale and much more.

Starting from the sensor (the load cell) and its specifications and ending with the digital filter implementation, this application note provides information about each feature of the weight scale and their importance in the application.

FIGURE 1: *Photo of the MCP3564 Weight Scale Demo, P/N ARD00906.*

WEIGHT SCALE SYSTEM DIAGRAM

Figure 1 shows the weight scale demo using the MCP3564 24-bit Delta-Sigma ADC. Figure 2 shows an example of weight scale system diagram, containing the front end load cell circuit, gain amplifier, MCP3564 Delta-Sigma ADC and PIC24 16-bit microcontroller (MCU).

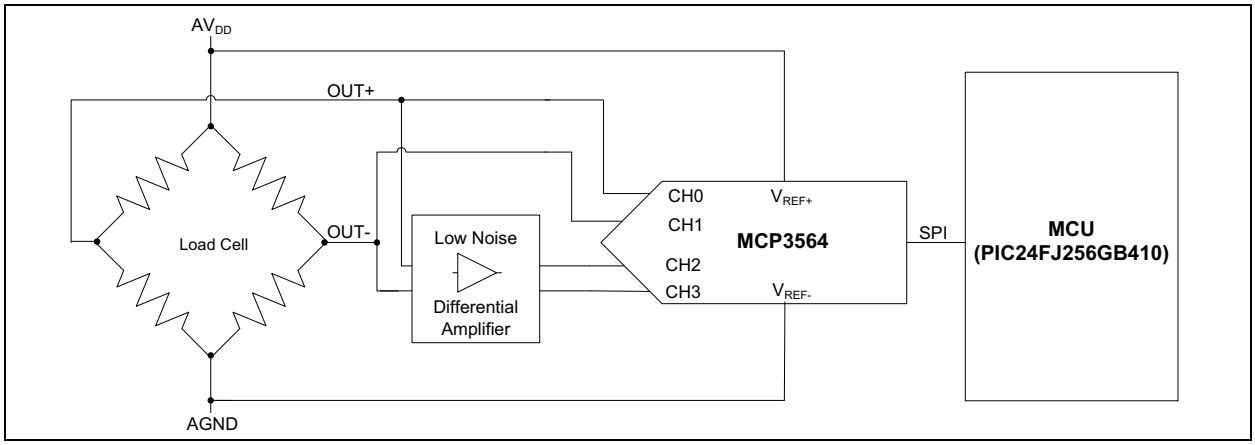

FIGURE 2: *Weight Scale Block Schematic.*

Load Cell

The most popular type of sensor for weight scales is the strain gauge load cell. The load cell is a transducer which converts an applied mechanical force into an electrical signal directly proportional with the magnitude of the force. The resistive load cell used in this application is composed of four strain gauges: two that measure tension and two that measure compression. These four strain gauges correspond to four resistors organized in a Wheatstone Bridge type of circuit, shown in Figure 3.

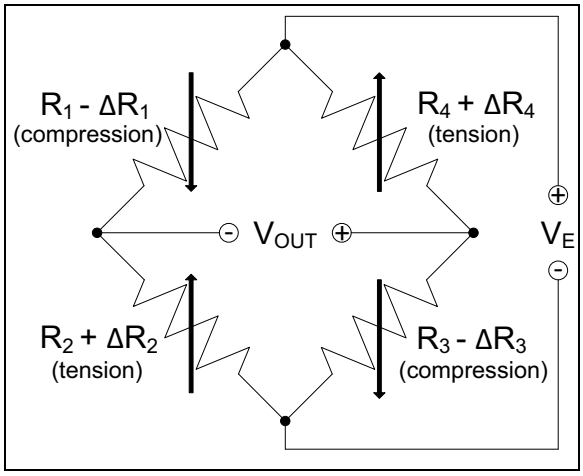

FIGURE 3: *Wheatstone Bridge Resistive Load Cell.*

The four strain gauges sense the bending contortion of the load cell under load translating to changes in the electrical resistances.

Power to the Wheatstone Bridge is supplied by a known excitation voltage (V_E) and its output voltage is defined by Equation 1.

EQUATION 1: WHEATSTONE BRIDGE OUTPUT VOLTAGE

$$V_{OUT} = \left[\frac{R_3}{R_3 + R_4} - \frac{R_2}{R_2 + R_1}\right] \times V_E$$

The bridge reaches a balanced state (V_{OUT} = 0) when no strain is applied (i.e. no load conditions). In this case, Equation 1 shows that the output voltage is null if: (R1/R2) = (R4/R3).

Any resistance variation in any arm of the bridge leads to an unbalanced state and to a nonzero output voltage. Ideally, if no strain is applied there is no variation in the resistances ($\Delta R_{1\text{-}4}$ = 0). In practice, these variations can occur due to changes in temperature load cell manufacturing imperfections and aging. These changes can lead to an offset output voltage which needs to be calibrated out of the system.

Other types of load cells have different strain gauge configurations. The one presented in Figure 3 is called a Full Bridge Configuration because it has four active elements (the strain gauges) which form the entire Wheatstone Bridge. There are two other types: quarter bridge and half bridge. The quarter bridge configuration has a single active strain gauge element, while the half bridge has two elements. The downside of these configurations is that additional passive elements (resistors) are required in order to complete the bridge.

The full bridge configuration load cell is more sensitive to bending contortion and less sensitive to temperature changes. The temperature change effect is more visible in the quarter and half bridge designs because the additional resistors used to complete the bridge will react to the temperature variation differently than the strain gauges, as they are made of different materials with different temperature tolerances.

One method of minimizing temperature effects is using the full bridge configuration where the strain gauges respond to temperature variations with the same change in resistance. This means that the ratios of the resistances are kept constant. Some load cells even have an additional resistive element which is not used for measuring the applied force. However, it is used in an instrumentation amplifier configuration as a gain setting resistor. This resistor will have a similar thermal coefficient as the resistive bridge and the temperature variation effect on output voltage will be minimized. This method was not investigated in this application note.

Another solution is to implement temperature drift correction using software, but the necessity of this software correction depends on the chosen load cell's specifications and the conditions in which the sensor is used. For instance, it is important to know the temperature operating range of the load cell and how thermally unstable the environment in which it is used/integrated will be. Also, the temperature effect on output is often specified in the sensor's specifications table and this gives the maximum difference in the output caused by a change in temperature of ±1°C, when the load remains constant. In addition, even using a high excitation voltage for the load cell could cause the sensor to overheat and affect the accuracy of the measurement. These aspects should be taken into consideration when deciding if a temperature drift software correction is required.

Table 1 shows the key specifications of the load cell used for this application.

TABLE 1: LOAD CELL SPECIFICATIONS

Specification Description	Specification Value	Specification Value for a Load Cell with a 2 kg Capacity
Output Sensitivity	1.0 ± 15% mV/V	
Safe Overload	150 %F.S(1)	3 kg
Maximum Overload	200 %F.S	4 kg
Nonlinearity	±0.05 %F.S	±1g
Non-repeatability		
Hysteresis		
Creep (5 min.)		
Temperature Effect on Output	±0.05 %F.S/°C	±1g/°C
Temperature Effect on Zero	±2.0 %F.S/°C	±40g/°C
Zero Balance	±10 %F.S/°C	±0.2 kg
Input/Output Resistance	1000 ± 10Ω	
Excitation Voltage	≤ 6V	
Operating Temperature Range	-10°C to +40°C	

Note 1: Where F.S is full scale.

The output of the Wheatstone Bridge composed of strain gauges is a very low-level voltage signal (typically in the range of µV to mV) which needs to be gain amplified before feeding into the ADC.

Equation 2 can be used to estimate the load cell output voltage range using Table 1. For example, the output sensitivity of the load cell used in this application is 1 mV/V. This means that when the excitation voltage is 3.3V, the output signal will be 3.3 mV at full load. Full load is the maximum capacity of the sensor, in this case 2 kg. Equation 2 shows that for a 1 gram load change the output will vary with 1.65 µV. This is a quick estimation before selecting a right load cell based on system requirements.

EQUATION 2: LOAD CELL OUTPUT VOLTAGE

$$V_{OUT} = \frac{Output\ Sensitivity[mV/V] \times Excitation\ Voltage[V]}{Maximum\ Capacity[g]} \times Load[g]$$

$$V_{OUT} = \frac{1\ mV/V \times 3.3V}{2000g} \times 1g = 1.65\ \mu V$$

Also, the capacity of the load cell should be selected carefully. If the maximum overload limit of the sensor is exceeded, it can be permanently damaged.

As mentioned before, a balanced state of the bridge is achieved when an excitation voltage is applied and there is no load. Under these conditions the output voltage of the bridge would ideally be 0V. In practice, the maximum output voltage deviation of the load cell from 0 is given by the Zero Balance and the Temperature Effect on Zero specifications of the sensor (See Table 1). This deviation can be corrected through offset calibration.

Sensor temperature drift can be corrected in software using a digital temperature sensor and a compensation algorithm which accounts for variation of the sensor output voltage over temperature. The Temperature Effect on Zero and Temperature Effect on Output specifications are key to implementing a compensation algorithm for the output voltage variation over temperature.

For adding extra precision and accuracy to a weight scale, a thermocouple can be used together with the digital temperature sensor. The thermocouple provides a voltage which is dependent on the temperature difference between its hot and its cold junction, but its output is in the µV range. Therefore, it requires amplification before converting the output to digital data. The digital temperature sensor can be used to measure the cold junction temperature. There are ADCs which provide both an analog gain stage and an internal temperature sensor, such as the MCP3564 ADC used in this application. The thermocouple can be connected directly to the converter without additional circuitry and the cold junction temperature can be estimated with this internal temperature sensor. However, an external digital temperature sensor, such as Microchip's MCP9800, is highly recommended as it increases the accuracy of the measurement.

Table 1 shows four other specifications which represent errors that can appear in the output of a non-ideal sensor.

- The nonlinearity parameter indicates the maximum deviation of the output curve from the ideal curve over the entire operating range.
- The non-repeatability specification is the maximum difference between load cell outputs for repeated measurements of the same weight and under the same conditions.
- The hysteresis effect can be observed by checking the difference in the output, measured once when the load increases from 0 up to a certain value and once when the load decreases from the maximum capacity down to that same value. There will be a difference between the two readings caused by hysteresis. It is important to note that the maximum value of this error is seen over the full range of the sensor and it decreases with smaller weight changes.
- Creep is defined as the change in the output when the load cell is under a fixed load for a certain period of time.

For the load cell used in this application, creep is computed over five minutes, as indicated in Table 1. This effect appears as a result of the load cell's material stretching over time while under the same load. Depending on the load and how deformable the material is, it may take a while for the load cell to recover after the load is removed assuming it hasn't been damaged. This change in output after the removal of the load is known as creep recovery and is specified in the specifications table for some load cells.

The simplest Wheatstone Bridge circuit is shown in Figure 4. The load cell output voltage needs to be converted to a digital value such that the data can be acquired and processed by the microcontroller. However, to get the best precision and ensure the accuracy of this measuring process other important aspects must be considered.

As previously stated, the load cell's output voltage needs to be amplified in order to take advantage of the full input span of the ADC and to get more accurate results. Since the bridge output is differential, a differential amplifier can be used prior to the ADC's input. Another option is using a high resolution ADC, such as the MCP3564, which can be connected directly to the Wheatstone Bridge without using additional front-end circuity. The differential input and the on-board programmable gain amplifier (PGA) of the MCP3564 make it ideal for this application as it eliminates any external circuitry which may be needed for Common-mode noise rejection or signal amplification on the front-end of the ADC.

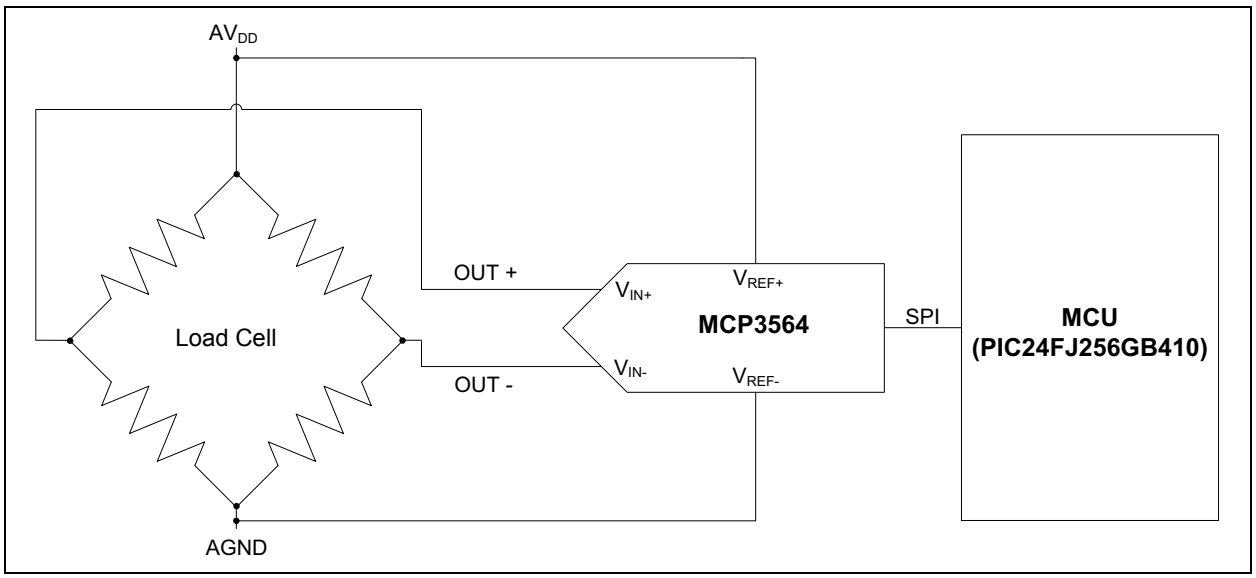

FIGURE 4: *Simplified Block Diagram of Weight Scale Measurement System.*

MCP3564 Delta-Sigma ADC Features

The MCP3564 Analog-to-Digital Converter utilizes an oversampling Delta-Sigma architecture to achieve a 24-bit resolution.

The MCP3564 offers eight single-ended and four differential analog input channels with a programmable gain stage with gain factors from 1/3x to 64x. In addition, the device has the option for differential reference voltage input. It also includes an internal oscillator, an internal temperature sensor and a burnout current source used for open/short circuit detection of external sensors.

When using differential inputs, the input signal is defined by Equation 3.

EQUATION 3: DIFFERENTIAL INPUT VOLTAGE

$$V_{IN} = V_{IN+} - V_{IN-}$$

Ideally, only the differential voltage seen between the $V_{IN}+$ and $V_{IN}-$ inputs would be amplified and converted and any Common-mode voltage seen at these inputs would be rejected. In reality, however, this is not the case. Any unwanted Common-mode voltages seen at the inputs would also be amplified before differentially converted. The Common-Mode Rejection Ratio (CMRR) of the device is an important specification which indicates a device's ability to reject these Common-mode voltages.

The Common-mode input voltage is defined by Equation 4.

EQUATION 4: COMMON-MODE INPUT VOLTAGE

$$V_{INCOM} = \frac{V_{IN+} + V_{IN-}}{2}$$

EQUATION 5: COMMON-MODE REJECTION RATIO

$$CMRR(dB) = 20log\left(\frac{\Delta V_{OUT}}{\Delta V_{INCOM}}\right)$$

Where:

V_{OUT} = the equivalent voltage of the ADC output code obtained with the ADC transfer function.

The CMRR specification values of the MCP3564 ADC are presented in Table 2. The DC CMRR is computed for a Common-mode input voltage which takes multiple DC values and the AC CMRR is computed for a Common-mode input voltage which is a sine wave.

TABLE 2: COMMON-MODE REJECTION

Parameters	Sym.	Min.	Typ.	Max.	Units	Conditions
DC Common-mode Rejection Ratio	DC CMRR	—	-126	—	dB	V_{INCOM} varies from 0V to AVDD V_{IN} = 0V
AC Common-mode Rejection Ratio	AC CMRR		-122			V_{INCOM} = 0 dB at 50 Hz V_{IN} = 0V

The MCP3564 also has configurable Oversampling Ratio (OSR), from 32 to 98304. This provides a method of trading data conversion speed for precision. Lower OSR is used for applications which need fast data rates but do not require high accuracy. Higher OSR values are used when the application requires higher accuracy but doesn't need high conversion speed.

Table 3 shows how the noise is influenced by the OSR and the GAIN values. Table 4 shows their impact on the Effective Number of Bits (ENOB). Here the results are not presented for all the possible OSR values, but only for some values distributed over its entire range.

The MCP3564 has an analog gain stage which can be configured from 1/3x to 16x, and a digital gain with a range between 1x and 4x. When gain values larger than 16x are selected, the analog gain stage stays constant at 16x and the extra gain is added in the digital domain. In Table 3 and Table 4, the gain is considered only up to 16x, because the digital gain does not change the noise performance significantly.

TABLE 3: NOISE RMS LEVEL VS. GAIN VS. OSR

Total OSR	RMS (Peak-to-Peak) Noise (µV)					
	GAIN = 0.33	GAIN = 1	GAIN = 2	GAIN = 4	GAIN = 8	GAIN = 16
32	365.02 (2932.548)	120.80 (981.899)	60.79 (489.771)	30.70 (243.707)	15.69 (125.985)	8.23 (65.940)
256	24.83 (212.312)	8.94 (73.354)	4.94 (40.625)	2.94 (23.384)	1.88 (15.173)	1.29 (10.109)
2048	11.47 (91.513)	4.08 (32.008)	2.26 (18.037)	1.34 (10.693)	0.86 (6.795)	0.59 (4.575)
16384	4.16 (30.557)	1.50 (10.805)	0.84 (6.122)	0.50 (3.650)	0.32 (2.285)	0.22 (1.596)
40960	2.70 (18.794)	0.98 (6.528)	0.55 (3.829)	0.32 (2.222)	0.20 (1.407)	0.14 (0.956)
98304	1.94 (12.198)	0.68 (4.367)	0.38 (2.387)	0.22 (1.370)	0.14 (0.893)	0.09 (0.588)

TABLE 4: EFFECTIVE NUMBER OF BITS

Total OSR	ENOB (Peak-to-Peak) RMS (bits)					
	GAIN = 0.33	GAIN = 1	GAIN = 2	GAIN = 4	GAIN = 8	GAIN = 16
32	15.7 (12.7)	15.7 (12.7)	15.7 (12.7)	15.7 (12.7)	15.7 (12.7)	15.6 (12.6)
256	19.6 (16.5)	19.5 (16.5)	19.4 (16.3)	19.1 (16.1)	18.7 (15.7)	18.3 (15.3)
2048	20.7 (17.7)	20.6 (17.7)	20.5 (17.5)	20.2 (17.2)	19.9 (16.9)	19.4 (16.5)
16384	22.2 (19.3)	22.1 (19.2)	21.9 (19.0)	21.6 (18.8)	21.3 (18.5)	20.9 (18.0)
40960	22.8 (20.0)	22.7 (20.0)	22.5 (19.7)	22.3 (19.5)	21.9 (19.2)	21.5 (18.7)
98304	23.3 (20.6)	23.2 (20.5)	23.1 (20.4)	22.8 (20.2)	22.5 (19.8)	22.1 (19.4)

Figure 5, Figure 6 and Figure 7 show the measurement distributions with different OSR settings. It can be easily noticed that the standard deviation (or random noises) decreases significantly with the increase of the Oversampling Ratio.

Using the weight scale's dedicated graphical user interface (GUI), the gain stage of the ADC and the OSR can be dynamically reconfigured and their effect on measurements can be analyzed. One of the most important parameters is the standard deviation. Standard Deviation quantifies the dispersion of the data values from a dataset and shows how the precision of the weight scale is influenced by the oversampling ratio with a fixed gain of 64x.

Equation 6 shows how the standard deviation is computed:

EQUATION 6: STANDARD DEVIATION

$$\sigma = \sqrt{\frac{\Sigma_{i=1}^{N} (x_i - \bar{x})^2}{N-1}}$$

Where:

- N = number of values in the dataset
- x_i = the i^{th} value from the dataset [{x_1, x_2,..., x_N} - dataset values]
- $\bar{x}$ = the mean of the values from the dataset

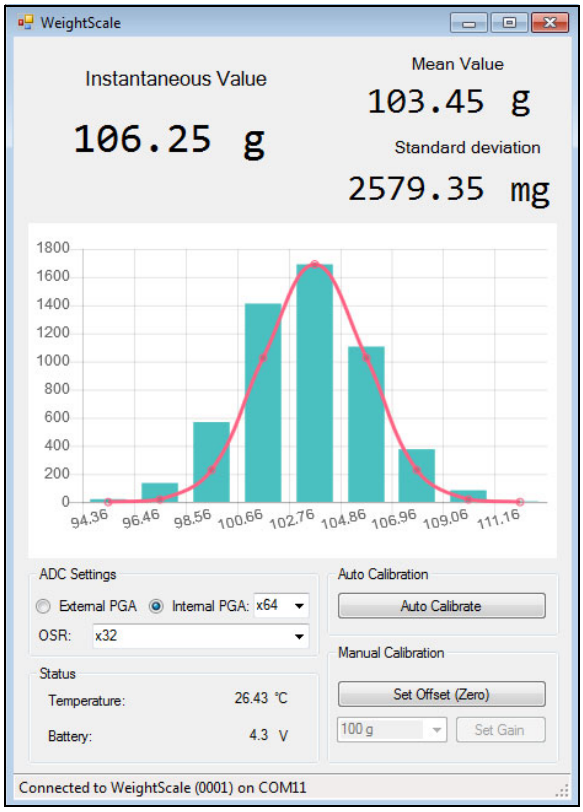

FIGURE 5: *PGA Gain = x64, OSR = 32.*

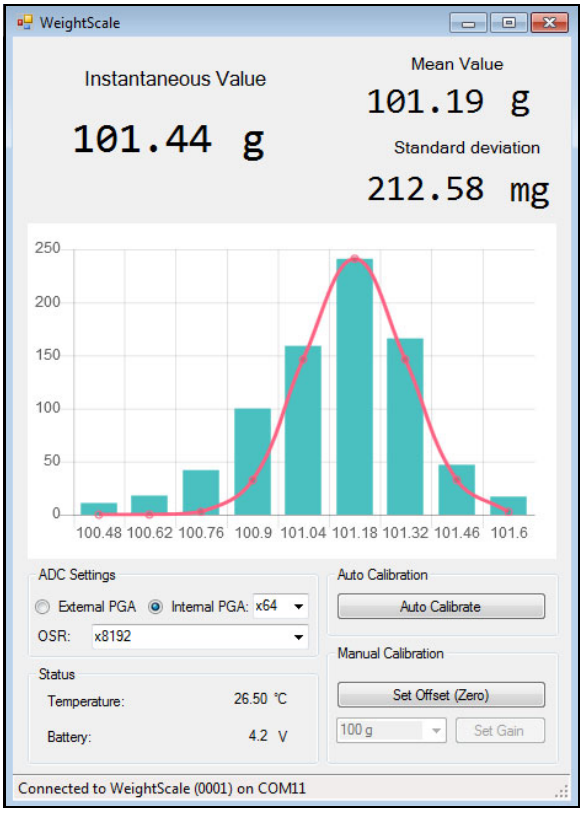

FIGURE 6: *PGA Gain = x64, OSR = 8192.*

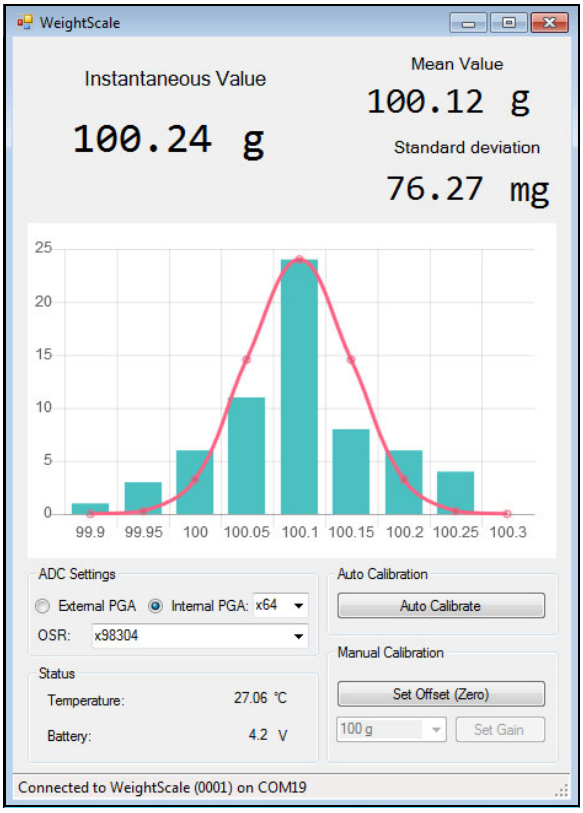

FIGURE 7: *PGA Gain = x64, OSR = 98304.*

Ratiometric Measurement

A ratiometric measurement is more suitable for a bridge-based sensor as it can improve the stability of the measurement and eliminates the problems introduced by a noisy voltage source.

The reference voltage of the ADC should be the same as the excitation voltage applied to the load cell. With this configuration the ADC output code will be a digital ratiometric representation of the input voltage relative to the ADC reference voltage (excitation voltage).

The advantage of a ratiometric measurement is that when the supply voltage varies, the output sensitivity mV/V ratio will remain constant. If the output sensitivity is 1 mV/V for a supply voltage of 3V, the output will be a 3 mV signal at full load (2 kg for the chosen load cell). Therefore, the fact that the output is ratiometric (the mV/V ratio is kept constant) implies a certain measurement stability. Any noise from the voltage supply, be it due to temperature variations or any other noise source, will not affect the measurement significantly.

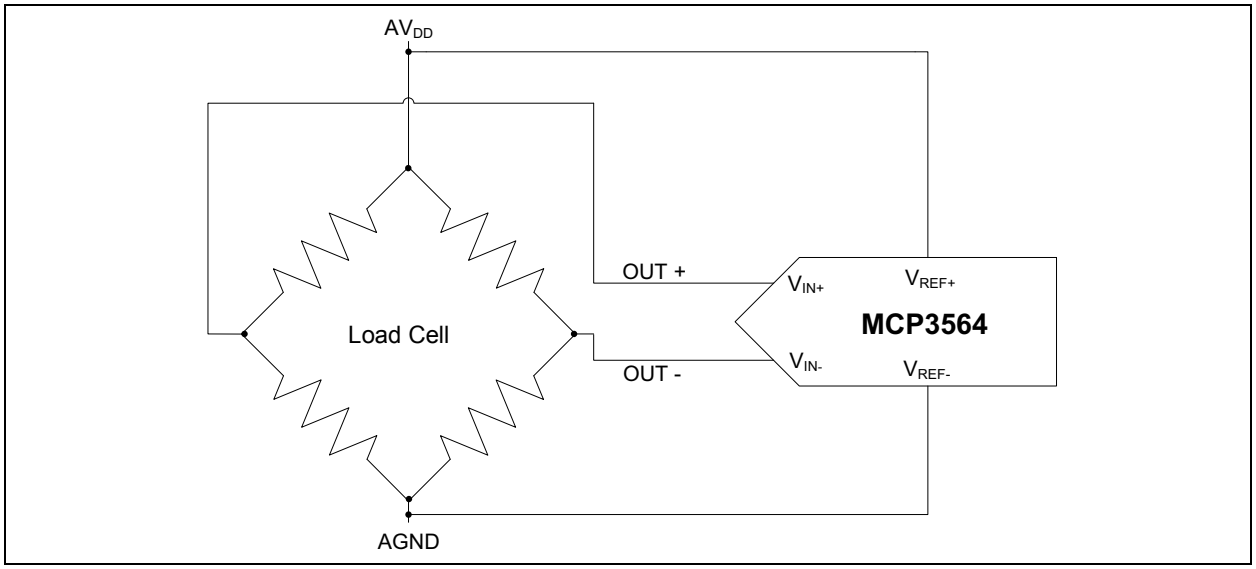

FIGURE 8: *Ratiometric Measurement Schematic.*

The ADC itself also has a Power Supply Rejection Ratio (PSRR) specification which characterizes the influence of the power supply noise on the ADC output codes.

EQUATION 7: POWER SUPPLY REJECTION RATIO

$$PSRR(dB) = 20log\left(\frac{\Delta V_{OUT}}{\Delta AV_{DD}}\right)$$

Where:

V_{OUT} = the equivalent voltage of the ADC output code obtained with the ADC transfer function

The PSRR is measured for multiple AC and DC values of the power supply. For AC measurements, a sine wave is used with its amplitude representing possible changes in the power supply. See Table 5 for more information regarding how the AC and DC PSRR values are determined.

TABLE 5: POWER SUPPLY REJECTION

Parameters	Sym.	Min.	Typ.	Max.	Units	Conditions
AV_{DD} Power Supply Rejection Ratio	DC PSRR	—	-76 dB + 20 x LOG(GAIN)	—	dB	
DV_{DD} Power Supply Rejection Ratio	DC PSRR		-110			DV_{DD} varies from 2.7V to 3.6V V_{IN} = 0V
AC Power Supply Rejection Ratio	AC PSRR		-75 dB - 20 x LOG(GAIN)			DV_{DD} = 3.3V AV_{DD} = 3.3V + 0.3VP, 50 Hz V_{IN} = 0V

For example, using the formula shown in Table 5 an AC PSRR of 99.08 dB can be calculated when assuming a gain of 16x is used:

$$\text{AC PSRR} = -75\ \text{dB} - 20 \times \log(16) = -99.08\ \text{dB}$$

Assuming a variation in the power supply of 100 µV, Equation 7 shows that:

$$\Delta V_{OUT} = 10^{(\text{PSRR (dB)}/20)} \times \Delta AV_{DD}\ (\mu V)$$

$$\Delta V_{OUT} = 10^{(-99.08\ \text{dB}/20)} \times 100\ \mu V = 1.1\ nV$$

This voltage is significantly lower than the amplified load cell's output voltage. Therefore, the measurement is not notably affected by the power supply noise.

NOTES:

FEATURES OF THE MCP3564 WEIGHT SCALE DEMO

External Low-Noise Differential Amplifier

To improve the accuracy and the precision of the measurement, the weight scale board demo includes an external low- noise differential amplifier (Figure 2). The external differential amplifier offers the ability to amplify the input signal (load cell output voltage) beyond the capability of the programmable gain stage of the ADC. The ADC's amplifier has a configurable gain range from 1/3x to 64x, whereas the external amplifier has a fixed gain of 100x. The differential amplifier uses the MCP6492 Zero Drift Op Amp for its high PSRR and CMRR capabilities. The MCP6V92 also provides input offset voltage correction, which improves the noise rejection.

Using the GUI, the external amplifier can be enabled or disabled to demonstrate its impact on the application measurements. The accuracy and the precision of the measurements can be compared while using the external or the internal amplifier. The results at different OSR values (when using the external amplifier) can also be compared.

Figure 9, Figure 10 and Figure 11 show how the standard deviation varies when using the external amplifier with an OSR of 32, 8192 and 98304 respectively. The offset and gain of the system were calibrated using a 100g load.

When comparing standard deviation values of Figures 5, 6 and 7 where the internal PGA setting of the ADC is used versus the external amplifier (Figures 9, 10 and 11) it can be seen the results are improved considerably when using the external amplifier.

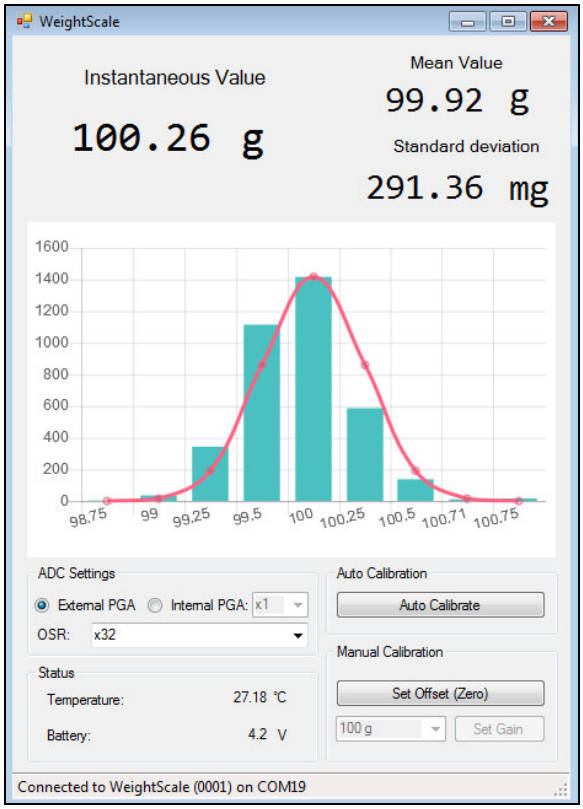

FIGURE 9: *External Amplifier, OSR = 32.*

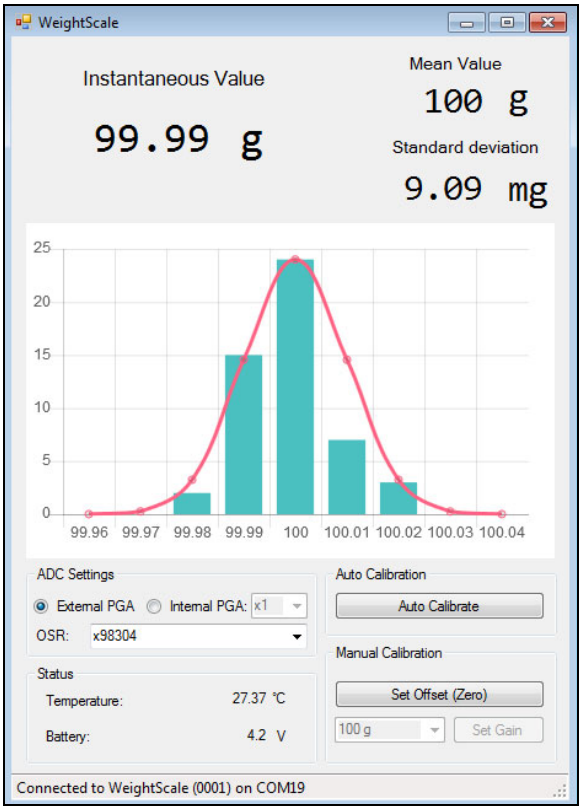

FIGURE 11: *External Amplifier, OSR = 98304.*

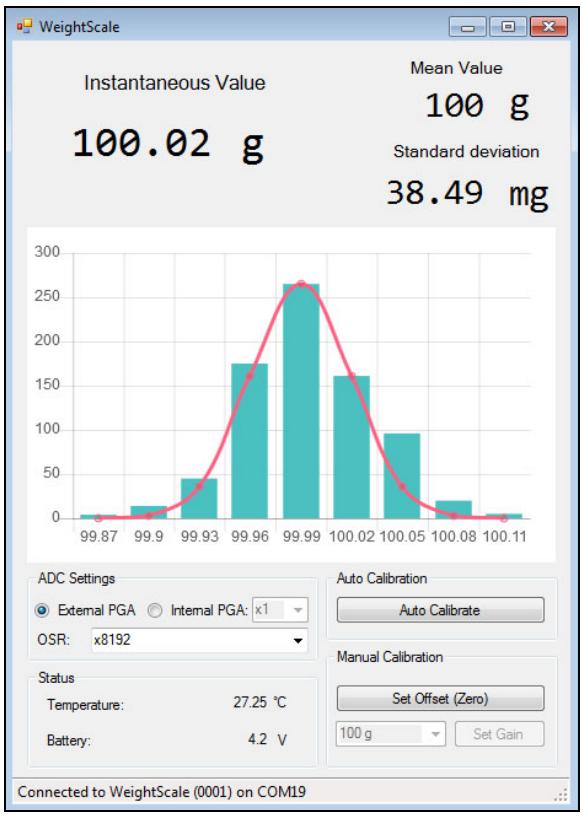

FIGURE 10: *External Amplifier, OSR = 8192.*

Ultra-Low Power Monitoring Amplifier

The ADC and the external low-noise op amp have significant current consumption during normal operation which will affect the lifetime of the battery. To minimize power consumption, the weight scale will enter a Low Power mode when not performing active weight measurements. In this mode, the weight scale will monitor if a mass is present by performing low-accuracy measurements periodically.

The weight scale has two operating modes: Run mode and Sleep mode. When the weight scale enters into Sleep mode, the microcontroller is awakened by the watchdog timer (WDT) at a predetermined time period to check if there was any load change using the “low-power” monitoring amplifier. If there is a significant change, the weight scale enters the Run mode. Otherwise, it goes back into Sleep mode.

When the weight scale enters Sleep mode, the ADC is disconnected. Instead of waking up the ADC, when checking for load variation, an ultra-low power monitoring amplifier is used.

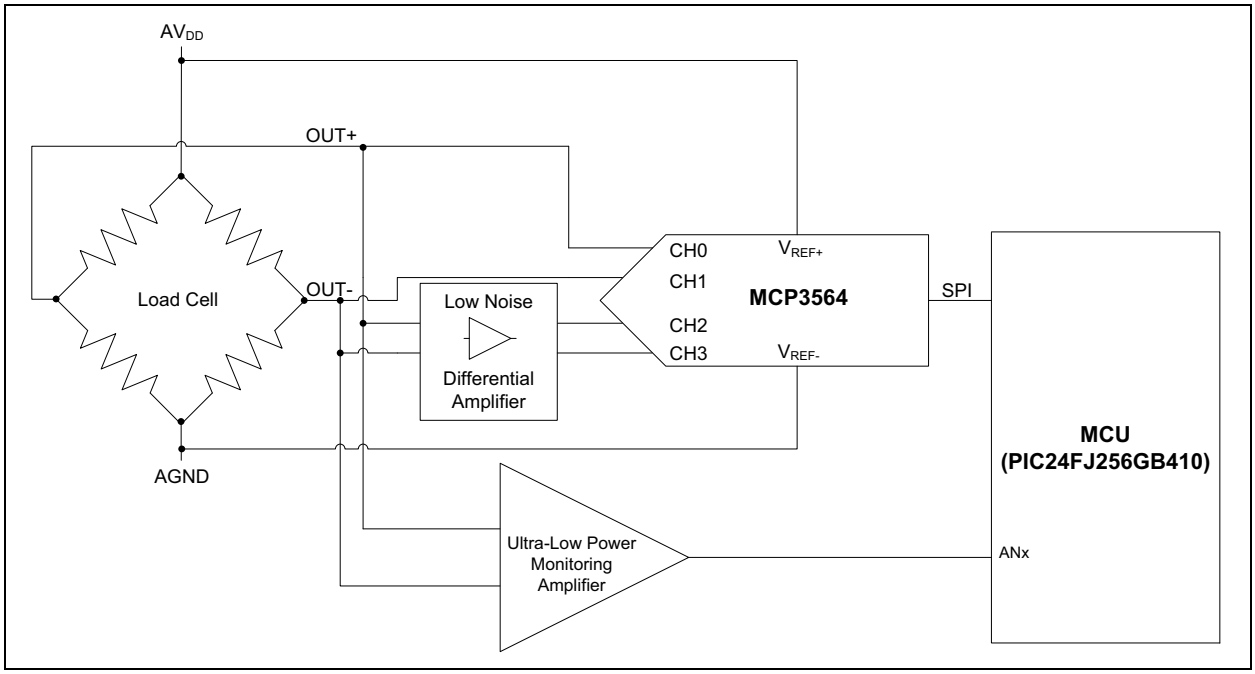

FIGURE 12: *Block Schematic with Ultra-Low Power Monitoring Amplifier.*

The Monitoring Amplifier uses the Microchip MCP6444 operational amplifier in an Instrumentation Amplifier configuration. The MCP6444 is a quad op amp with a quiescent current of 450 nA/op amp, suitable for usage in low power applications. The monitoring amplifier has a single ended output and can be connected directly to an analog input pin of the microcontroller. Its output voltage is converted using the PIC24's internal 12-bit ADC and compared to the value acquired at the previous wake-up event of the microcontroller. If there is a significant difference between the two values, the weight scale enters Run mode. Otherwise, the microcontroller goes back to Deep Sleep mode. For storing the measured value at each microcontroller wake-up, the Deep Sleep Semaphore registers (DSGPR0 and DSGPR1) are used since they are the only registers preserved in Deep Sleep. One is used for saving the value and the other is used as a flag to indicate if there was a previous measurement or not. These registers are reset every time the weight scale goes from Run mode to Sleep mode.

Another design option is to connect the amplifier to a comparator input. PIC24F devices include three dual-input comparators with selectable inputs from the analog inputs multiplexed with the I/O pins, as well as the on-chip voltage reference.

Even though the SAR ADC of the PIC24F devices is less accurate and less precise than using the MCP3564 ADC, it is good enough to detect a load change and to decide whether the entire device should wake up and get into the Run mode or if it should go back into Sleep mode.

The biggest advantage of using this monitoring amplifier is that it draws less current than the MCP3564 ADC (when in the Conversion operating mode), which leads to extended battery life.

Figure 13 shows the final block schematic of the MCP3564 Weight Scale Demo.

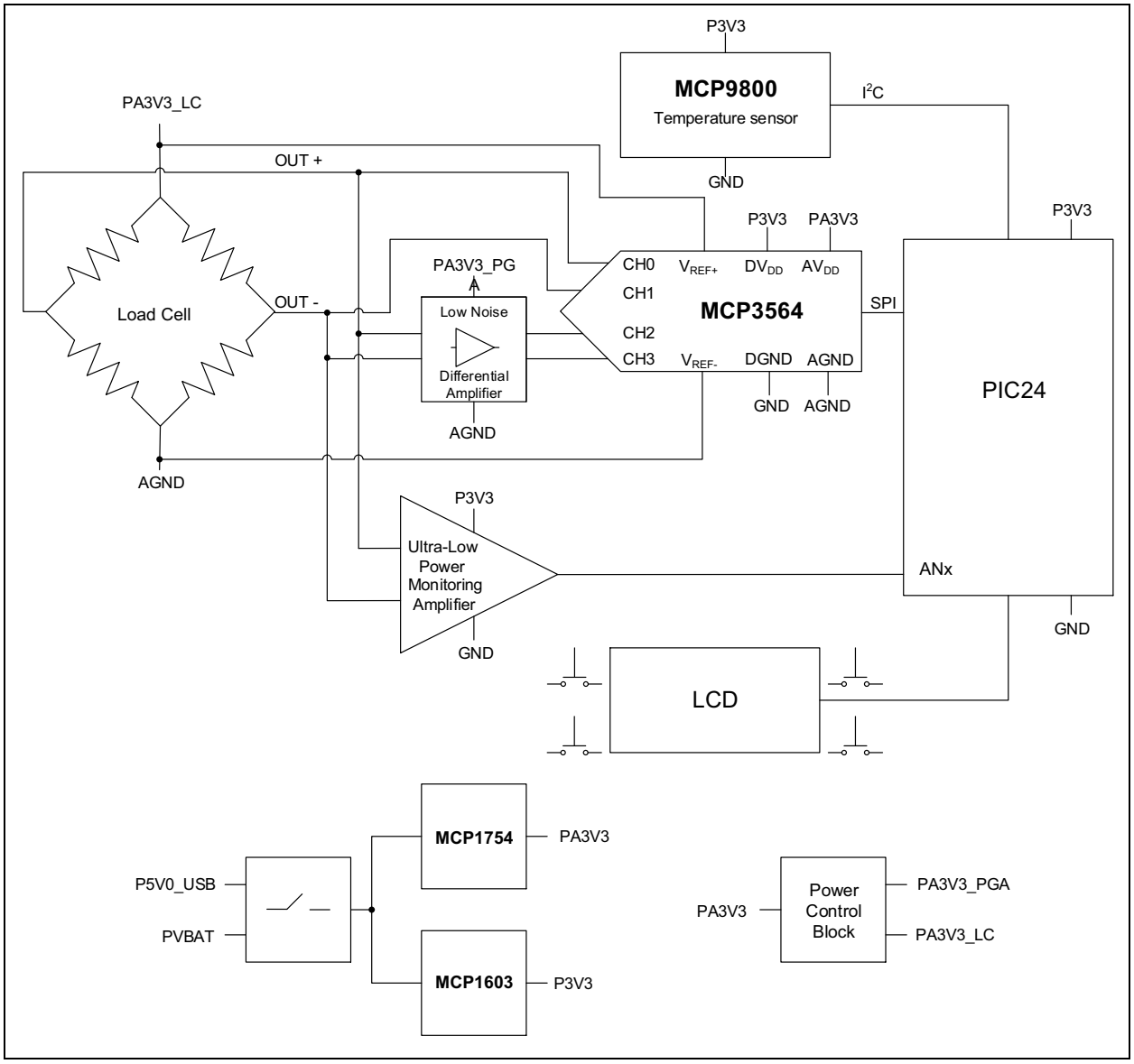

FIGURE 13: *Final Block Schematic.*

Temperature Sensor

Microchip's MCP9800 is a digital temperature sensor which allows the configuration of the temperature measurement resolution, the operating modes or the specification of both temperature alert output and hysteresis limits.

The MCP9800 has two power-saving operating modes: Shutdown and One-shot (single conversion on command then returns into Shutdown mode), both useful for keeping the weight scale's power usage low. The MCP9800 communicates with the microcontroller through the I^2C interface.

The measured temperature can be seen on the LCD by parsing through the menu or by checking it in the GUI. This sensor can be used to observe if and how the weight measurement noise is affected by the increase or decrease in temperature.

For a high precision weight scale design, the data from the MCP9800 can be used to compensate the temperature drift of the load cell's output. As previously discussed, a more accurate temperature drift correction is obtained when using a thermocouple together with this digital temperature sensor (used for cold junction measurement).

Microcontroller - PIC24FJ256GB410

The microcontroller used in this application is Microchip's PIC24FJ256GB410, a 16-bit microcontroller which offers some key features for this application.

The Extreme Low Power (XLP) Features, more specifically the extreme low power current consumption for Deep Sleep, is very useful as the power consumption can be minimized while the weight scale is not actively performing measurements. The XLP features are therefore excellent for extending battery life in battery powered applications.

The on-chip Watchdog Timer (WDT) is needed to wake up the microcontroller from Deep Sleep to check if there is any change in the load cell output. Another key feature of this microcontroller is the Liquid Crystal Display (LCD) module which allows choosing a low power LCD without a dedicated driver.

The MCP3564 is initialized, reconfigured, and read via the SPI interface using the PIC24F microcontroller.

LCD Glass

Using the LCD module of the microcontroller is very convenient for a low power application. By using a simple LCD glass, instead of a display with its own driver, power consumption can be significantly lowered. The LCD driver module can be used to generate the timing control to drive static or multiplexed LCD panels with up to 8 Commons and up to 64 Segments. The LCD glass used in this application uses 4 Commons and 25 Segments to display 6 main, and 4 secondary, digits along with the units of measurement, i.e. g or kg.

The LCD is used to display a menu. By navigating through this menu, the user can see:

- the measured weight in grams (Figure 14) and in kilograms (Figure 15),
- the calibration menu option (Figure 16),
- the temperature (Figure 17),
- the power supply voltage (Figure 18).

The power supply voltage is measured using a resistive divider and the microcontroller's internal SAR ADC. It is useful for checking if the batteries should be replaced.

The bottom right (SW201) and left (SW202) push-buttons can be used to navigate through the menu. The top left button (SW203) is used for choosing between the external or the ADC's internal amplifier. The top-right push-button (SW200) is used for auto-calibration when in the Calibration Menu state or, otherwise, only for offset calibration.

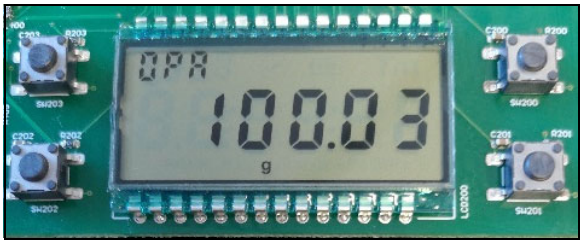

FIGURE 14: *LCD Menu - Grams.*

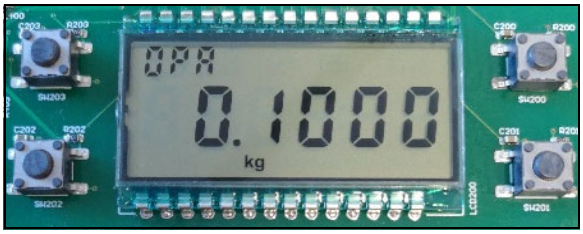

FIGURE 15: *LCD Menu - Kilograms.*

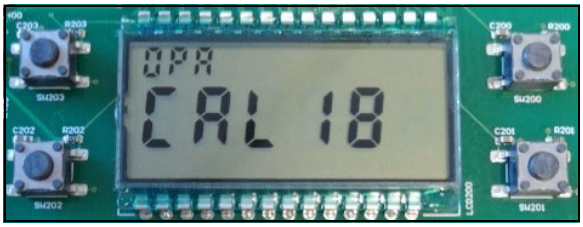

FIGURE 16: *LCD Menu - Calibration.*

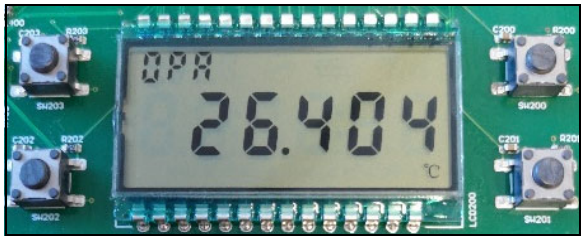

FIGURE 17: *LCD Menu - Temperature.*

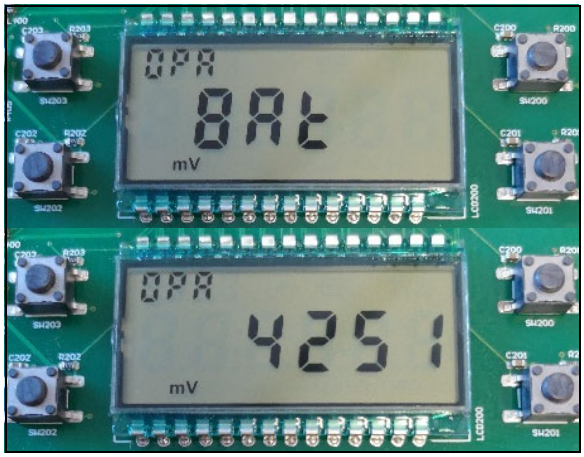

FIGURE 18: *LCD Menu - Power Supply Voltage.*

Power

The weight scale can be powered using the on-board triple-A battery socket or by way of the USB connector at J400.

An alternative to triple-A batteries could be a rechargeable lithium-polymer (LiPo) battery with a better weight-to-power ratio. A drawback to this alternative, however, is an increased cost which may be undesirable depending on the design constraints. For recharging the LiPo battery when the USB is connected, a battery charge management controller can be integrated in the design. For example, Microchip's MCP73830 provides specific algorithms developed to achieve optimal capacity and safety and to shorten the charging time as much as possible.

To reduce the overall system noise, separate analog and digital power supplies should be used. Microchip's MCP1754 is used for the analog circuitry and the MCP1603 is dedicated to the digital section. The MCP1754 is a low-dropout (LDO) voltage regulator with a typical quiescent current of 56 uA and a typical 300 mV dropout voltage. The MCP1603 is a synchronous buck regulator with a 2.7V to 5.5V input range and a typical quiescent current of 45 µA. Both regulators have shutdown control pins, another feature that makes them suitable for battery powered applications.

Due to the inherent sensitivity of analog circuitry, an LDO with high PSRR is highly desirable. For this reason the MCP1754 was selected for this application. The MCP1754 LDO has a typical PSSR of 72 dB at 1 kHz and a low output noise of 3 µV/√Hz.

A Power Control Block has been implemented to enable or disable the power supply to the load cell and external amplifier as needed. It can be controlled by the microcontroller in order to lower the power consumption when these components are not in use.

NOTES:

OFFSET AND GAIN ERROR CALIBRATION

In addition to the inherent offset of the sensor previously discussed, the design of the weight scale also implies an offset introduced by the weight tray. Furthermore, both the ADC itself and the external differential amplifier introduce additional offset and gain errors. Regarding the ADC, these errors vary with the GAIN and OSR settings and they have different values from device to device.

The gain error indicates the difference between the slope of the actual transfer function compared to the ideal one, defined by Equation 8.

EQUATION 8: ADC OUTPUT

$$ADC\_OUTPUT(LSB) = \left(\frac{V_{IN+} - V_{IN-}}{V_{REF+} - V_{REF-}}\right) \times 8388608 \times GAIN$$

A significant advantage of the MCP3564 ADC is that it provides digital calibration for offset and gain errors. This considerably reduces the amount of computations done in the microcontroller.

Equation 9 shows how the ADC output code (stored in the ADCDATA register) is modified with the offset and gain calibration values. These values are computed in the microcontroller and then written in the ADC's OFFSETCAL and GAINCAL 24-bit registers.

EQUATION 9: CALIBRATED ADC DATA

$$ADCDATA(post\text{-}calibration) = [ADCDATA(pre\text{-}calibration) + OFFSETCAL] \times GAINCAL$$

The MCP3564 also has two calibration control bits: EN_OFFCAL and EN_GAINCAL (see CONFIG3 register in the MCP3564 data sheet). When these bits are enabled, the values stored in the OFFSETCAL and GAINCAL registers are used to adjust the ADC output code. Otherwise, the calibration is not performed. One can choose to use only offset or only gain calibration and this can be done by enabling the corresponding control bit.

There are two ways to calibrate the weight scale: Manual or Auto-Calibration. Auto-Calibration can be done either by using the LCD menu and the physical buttons on the board or by using the GUI. For Auto-Calibration the user has to place the standard 100g weight on the weight scale tray.

If another weight value for gain calibration is preferable, manual calibration can be used and this is available only via the GUI. For manual calibration, there are two buttons, one for setting the offset and one for setting the gain. In this case, the gain calibration weight value can be chosen from a drop-down list (50g, 100g, 200g, 500g, 1000g) (see Figure 19).

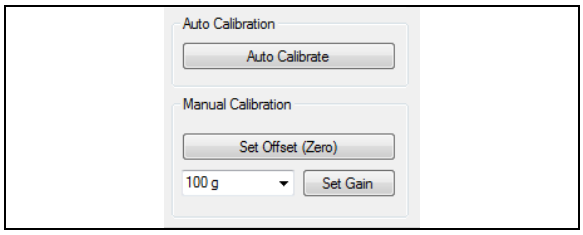

FIGURE 19: *Calibration Options.*

When the weight scale is powered up for the very first time, it requires gain and offset calibration. The message printed on the LCD is shown in Figure 20.

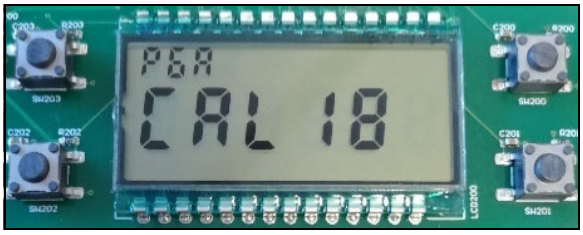

FIGURE 20: *Auto-Calibration - Start.*

The auto-calibration process can be started by pressing the top right button (SW200) on the board or the "Auto Calibrate" button from the GUI. The algorithm starts with the offset calibration. Two messages are displayed on the LCD to let the user know that the offset calibration has begun and the tray should be empty (see Figure 21).

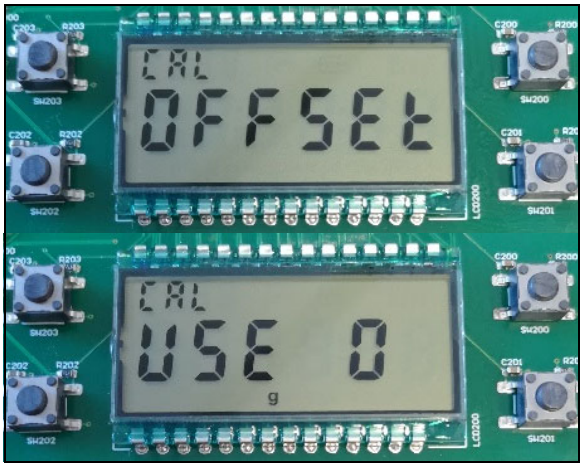

FIGURE 21: *Auto-Calibration - Offset.*

The algorithm detects when the load cell signal is stable enough in order to compute the offset and correspondingly set the ADC's offset calibration register. During this time, the display shows a loading bar to indicate that the offset calibration is still in progress (see Figure 22).

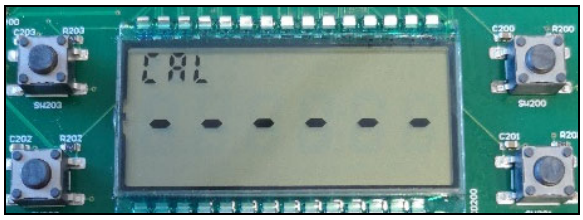

FIGURE 22: *Auto-Calibration - In Progress.*

After the stability detection is done and after the OFFSETCAL register is set, the process continues with the gain calibration. Two messages are displayed on the LCD to inform the user that the gain calibration process has begun and that the standard 100g weight needs to be placed on the tray (see Figure 23).

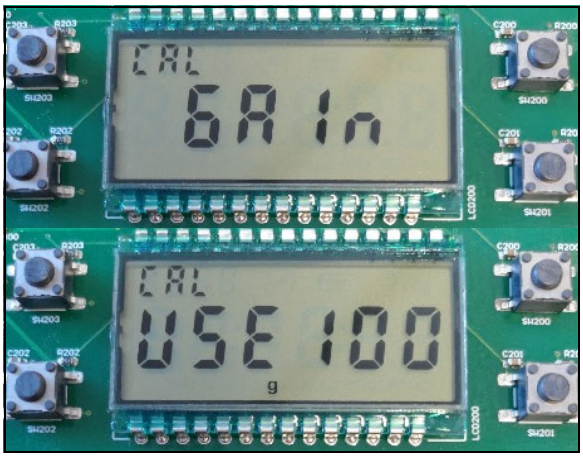

FIGURE 23: *Auto-Calibration - Gain.*

The next steps are signal stability detection and computation of the gain calibration value. Finally, after setting the gain calibration register (GAINCAL), the auto-calibration algorithm is done and the display will show the weight in grams.

After the initial calibration, the offset and gain calibration values are kept in the flash memory of the microcontroller, so the device does not need to be calibrated at each power up. Nevertheless, weight scale offset and gain calibration can be done at any time, either by using the LCD menu and the physical buttons or by using the user interface.

DIGITAL LOW-PASS FILTER

In order to reduce the noise level in the measurements even further, a software digital filter is implemented. The Low-Pass Filter (LPF) does a weighted average of the current input values and the previous ones. The implementation of its discrete form is based on Equation 10.

Depending on the Low-Pass Filter coefficient value, the previous values have a higher or a lower impact on the current output. Figures 24 to 29 show a comparison between filter outputs for different LPF coefficients when the load changes by 1 gram. For a low LPF coefficient (Figure 23 and Figure 24) the input variations are slightly attenuated, while for a higher value, it can be noticed that the filter smooths out the noisy input. As the coefficient increases, the current input value has a smaller impact on the output.

This is why the slope at the rising edge is less and less steep. This increases the precision, but the disadvantage of a high LPF coefficient is that it takes a longer time to notice load changes and for the output of the filter to increase or decrease to a certain value (Figure 27 and Figure 28). It also increases the time of the calibration process, as the algorithm waits for the signal to become stable.

Figure 25 and Figure 26 show an example of input filtering based on a good trade-off between the steepness of the slope (how fast the device reacts to load changes) and the precision of the measurement.

EQUATION 10: LOW-PASS FILTER EQUATION

$$y(n) = y(n-1) + \left(\frac{1}{2^{LPF\_coefficient}}\right) \times [x(n) + x(n-1) - 2 \times y(n-1)]$$

Where:

- $y(n)$ = filter output value
- $y(n - 1)$ = previous filter output value
- $x(n)$ = current weight value
- $x(n - 1)$ = previous weight value

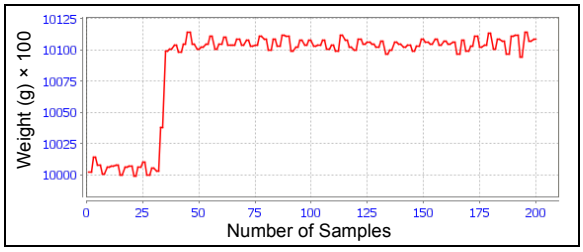

FIGURE 24: *Unfiltered Data, LPF Coefficient = 2.*

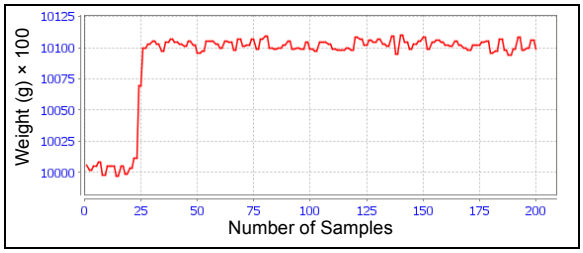

FIGURE 25: *Unfiltered Data, LPF Coefficient = 4.*

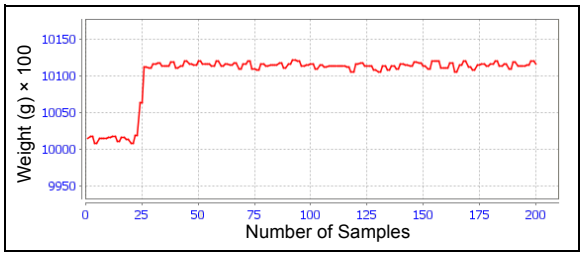

FIGURE 26: *Unfiltered Data, LPF Coefficient = 6.*

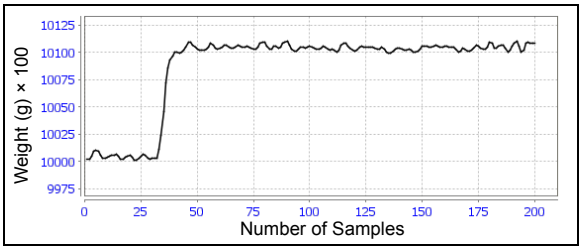

FIGURE 27: *Filtered Data, LPF Coefficient = 2.*

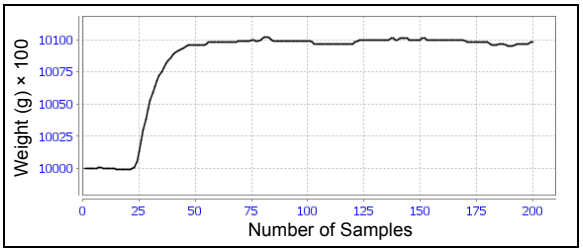

FIGURE 28: *Filtered Data, LPF Coefficient = 4.*

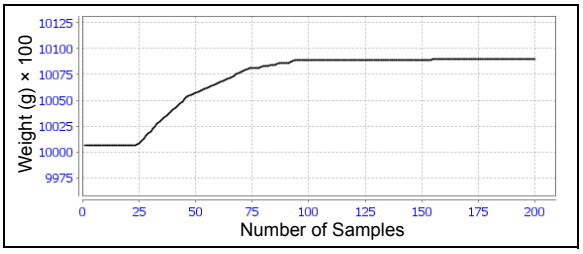

FIGURE 29: *Filtered Data, LPF Coefficient = 6.*

OPERATING MODES

The weight scale has two power modes: USB and Low Power Battery mode. When the USB is connected, it supplies the entire board and the device is up and running at all times. When the USB is disconnected, the batteries supply the device. In this case, good power management is required in the interest of prolonging the batteries' lifespan.

The operating states of the weight scale are:

- Run mode
- Sleep mode

Run Mode

Figure 30 represents the flowchart of the Run mode. The first step is to check whether the USB is connected or not in order to establish which power mode the device is using.

In both power modes, the weight scale acquires data (weight, temperature, power supply voltage) and displays it on the LCD, depending on the state in which the LCD menu is in. If any button event occurs, the corresponding command is executed.

In USB Power mode, the acquired data is not only displayed on the LCD, but also sent to the GUI. As shown before, by using this graphical user interface the user can monitor the instantaneous, mean and standard deviation weight values. Additionally, the temperature and battery voltage are shown. The Oversampling-Ratio (OSR) of the ADC can also be set via the user interface (GUI). The user can choose between the external or the internal amplifier. When using the internal amplifier the gain can be selected from the list of available values.

In Low Power Battery mode a timer is used to know how much time has passed since the last event has occurred, be it a button press or a significant load change. If the device has had no activity for 60 seconds, it enters into Sleep mode.

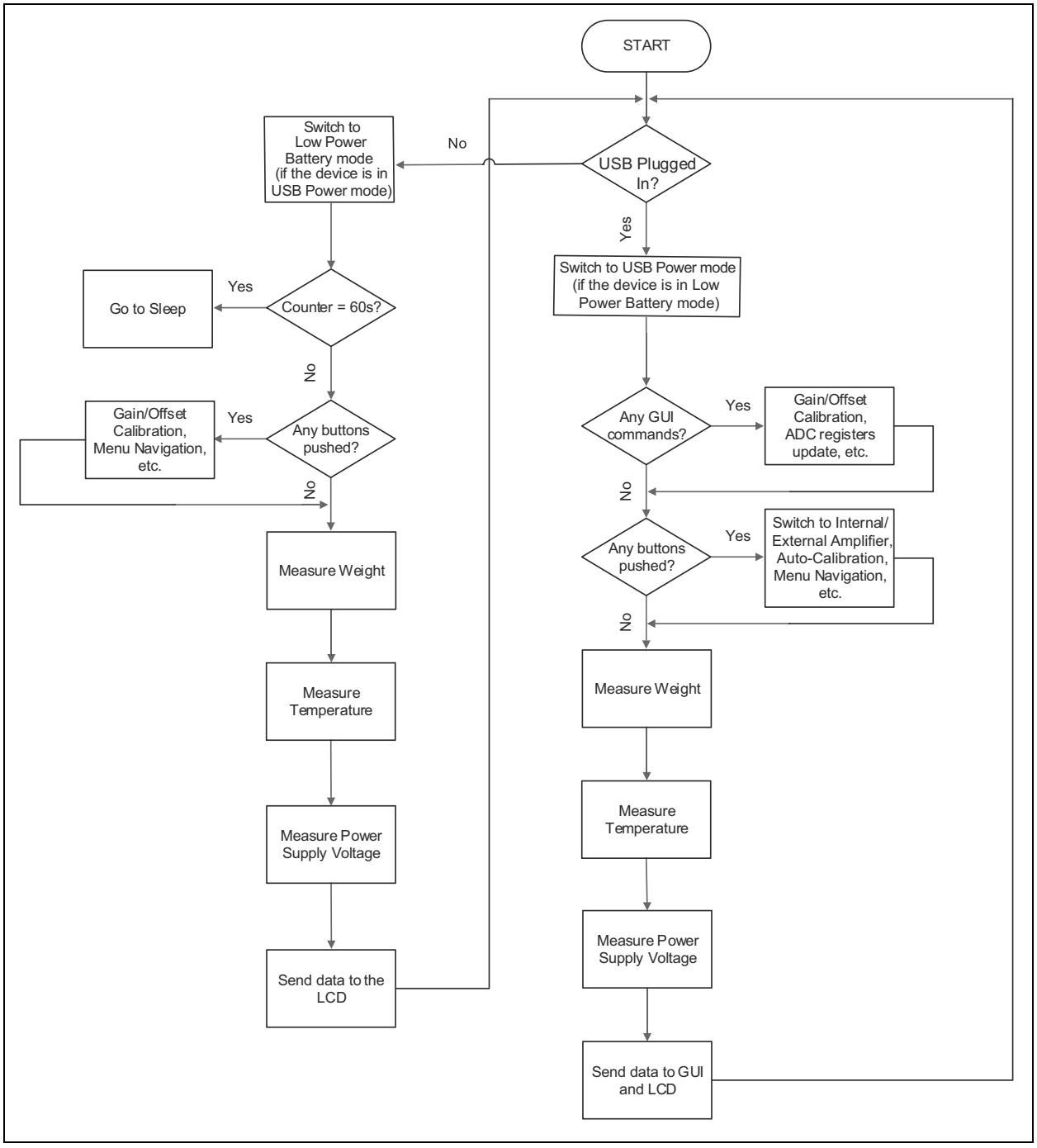

FIGURE 30: *Run Operating Mode Flowchart.*

Sleep Mode

Figure 31 shows the flowchart for the Sleep mode. When the device is in Sleep mode, the MCP9800 temperature sensor and the MCP3564 ADC stay in shutdown, along with the MCP1754 LDO and the MCP1603 buck regulator. After this step, the microcontroller enters into Deep Sleep mode.

The Deep Sleep watchdog timer uses the MCU's internal low power RC oscillator and is configured to wake up the MCU after approximately 500 ms of Deep Sleep. Even if MCP1603 is shut down and there is no power to the MCU, its output capacitor does not allow the MCU supply voltage to decrease below the lowest accepted V_{DD} value. The MCU is awakened by the watchdog timer, which in turn wakes up the buck regulator before the voltage on the output capacitor becomes too depleted.

When the PIC24 is in the Run mode, it also enables the LDO and the power control block in order to supply power to the load cell. The monitoring amplifier is used to check if there is any significant change in the load cell output voltage, in which case the device enters the Run Mode. Otherwise, the load cell's power supply is switched off, the buck regulator is shut down and the MCU goes back into Deep Sleep again, with the entire system remaining in Sleep mode.

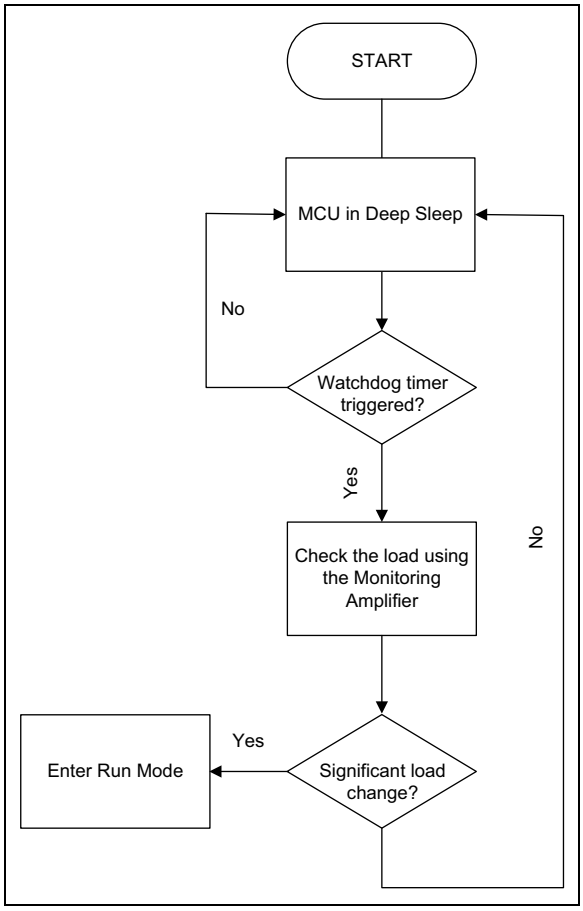

FIGURE 31: *Sleep Operating Mode Flowchart.*

NOTES:

CONCLUSION

This application note emphasizes the factors which impact the precision and the accuracy of a weight scale and provides solutions and methods for obtaining low noise measurements and a low power consumption of the entire system.

The load cell's specifications need to be well understood in order to appropriately decide what type of ADC should be used and whether the design requires an external amplifier or temperature compensation.

The weight scale application is based on the MCP3564 ADC, which has several advantages for weight scale type system design:

- configurable OSR and gain
- high PSRR and CMRR
- differential analog inputs (this allows direct connection of the Wheatstone Bridge)
- differential reference voltage inputs
- on-chip offset and gain calibration.

High OSR and gain values, as well as using the external low-noise differential amplifier, increase the precision and the accuracy of the measurements. Furthermore, by implementing and using the digital low-pass filter, a standard deviation of 0.02g can easily be achieved.

Using the PIC24FJ256GB410 microcontroller, with its XLP features proved advantageous for obtaining low power consumption. To save battery power, this application also includes an algorithm which switches the weight scale operating mode from Run mode to Sleep mode and an ultra-low power monitoring amplifier. At the expense of increasing the overall cost, using a LiPo battery and a charger are recommended for a different design if a better weight/power ratio is desired.

REFERENCES

[1] MCP3561/2/4 Data Sheet, "*Two/ Four/ Eight-Channel, 153.6 kSPS, Low-Noise 24-bit Delta-Sigma ADCs*", 2019 Microchip Technology, Inc.

[2] PIC24FJ256GA412/GB412 FAMILY Data Sheet, "*16-Bit Flash Microcontrollers with Dual Partition Flash Memory, XLP, LCD, Cryptographic Engine and USB On-The-Go*", 2015-2016 Microchip Technology Inc.

[3] MCP6V91/1U/2/4 Data Sheet, "*10 MHz, Zero-Drift Op Amps*", 2015-2016 Microchip Technology Inc.

[4] MCP6441/2/4 Data Sheet, "*450 nA, 9 kHz Op Amp*", 2010-2012 Microchip Technology Inc.

[5] MCP9800/1/2/3 Data Sheet, "*2-Wire High-Accuracy Temperature Sensor*", 2010 Microchip Technology Inc.

[6] MCP1603/B/L Data Sheet, "*2.0 MHz, 500 mA Synchronous Buck Regulator*", 2007-2012 Microchip Technology Inc.

[7] MCP1754/MCP1754S Data Sheet, "*150 mA, 16V, High-Performance LDO*", 2011-2013 Microchip Technology Inc.

NOTES:

APPENDIX A: SCHEMATICS AND LAYOUT

This appendix contains the schematic and the layout of the MCP3564 Weight Scale Board.

A.1 Weight Scale Board - Schematic 1

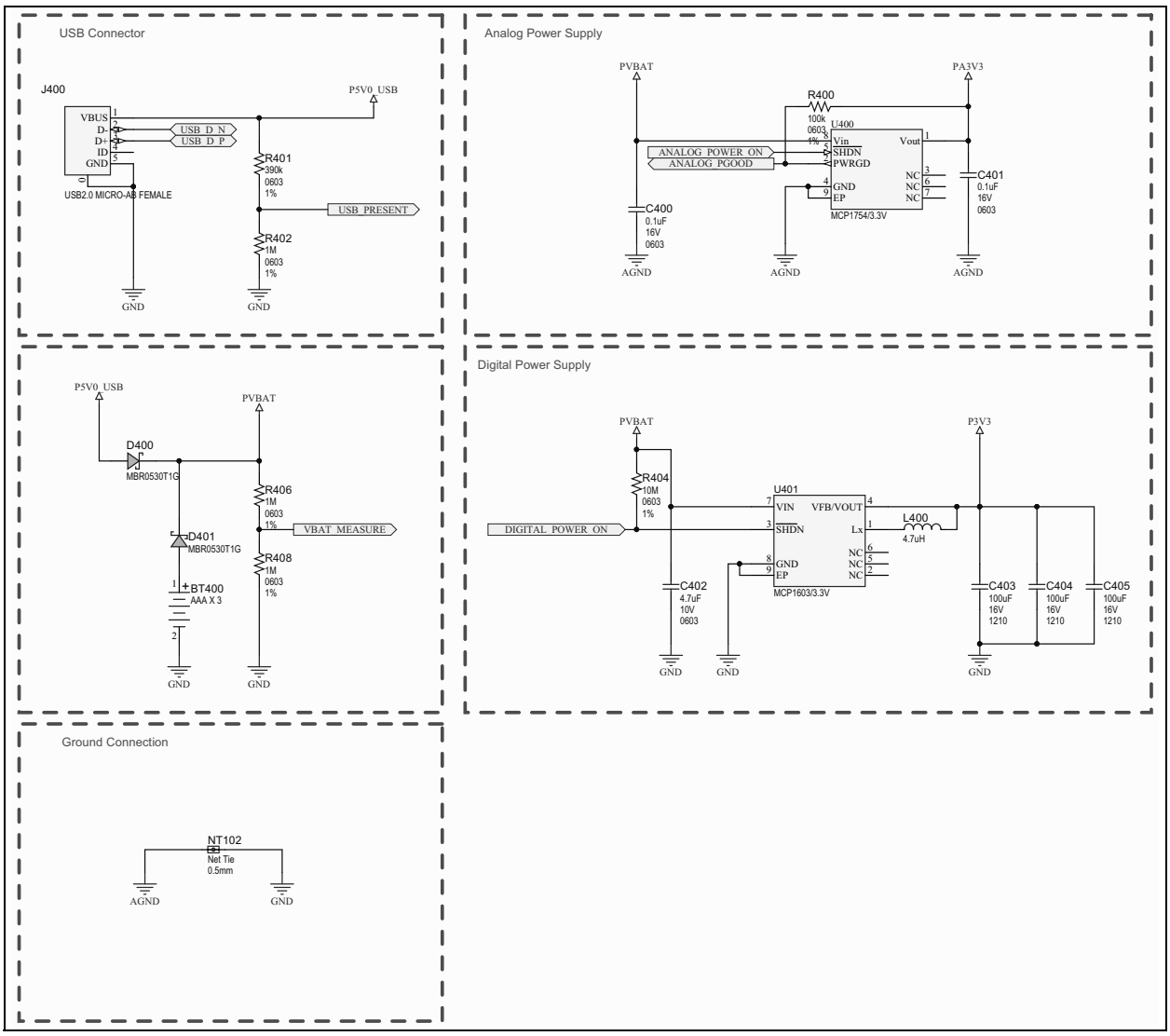

A.2 Weight Scale Board - Schematic 2

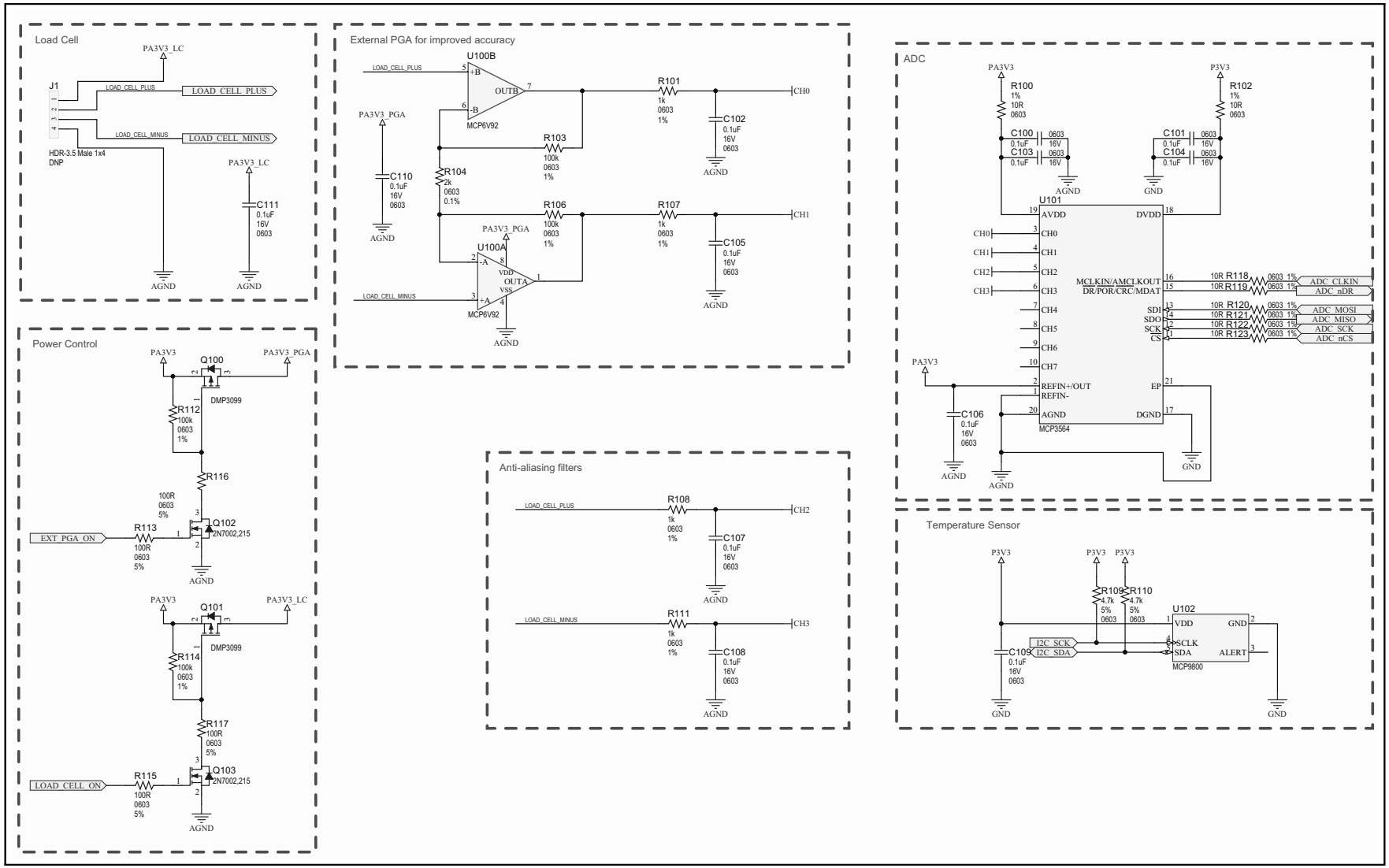

A.3 Weight Scale Board - Schematic 3

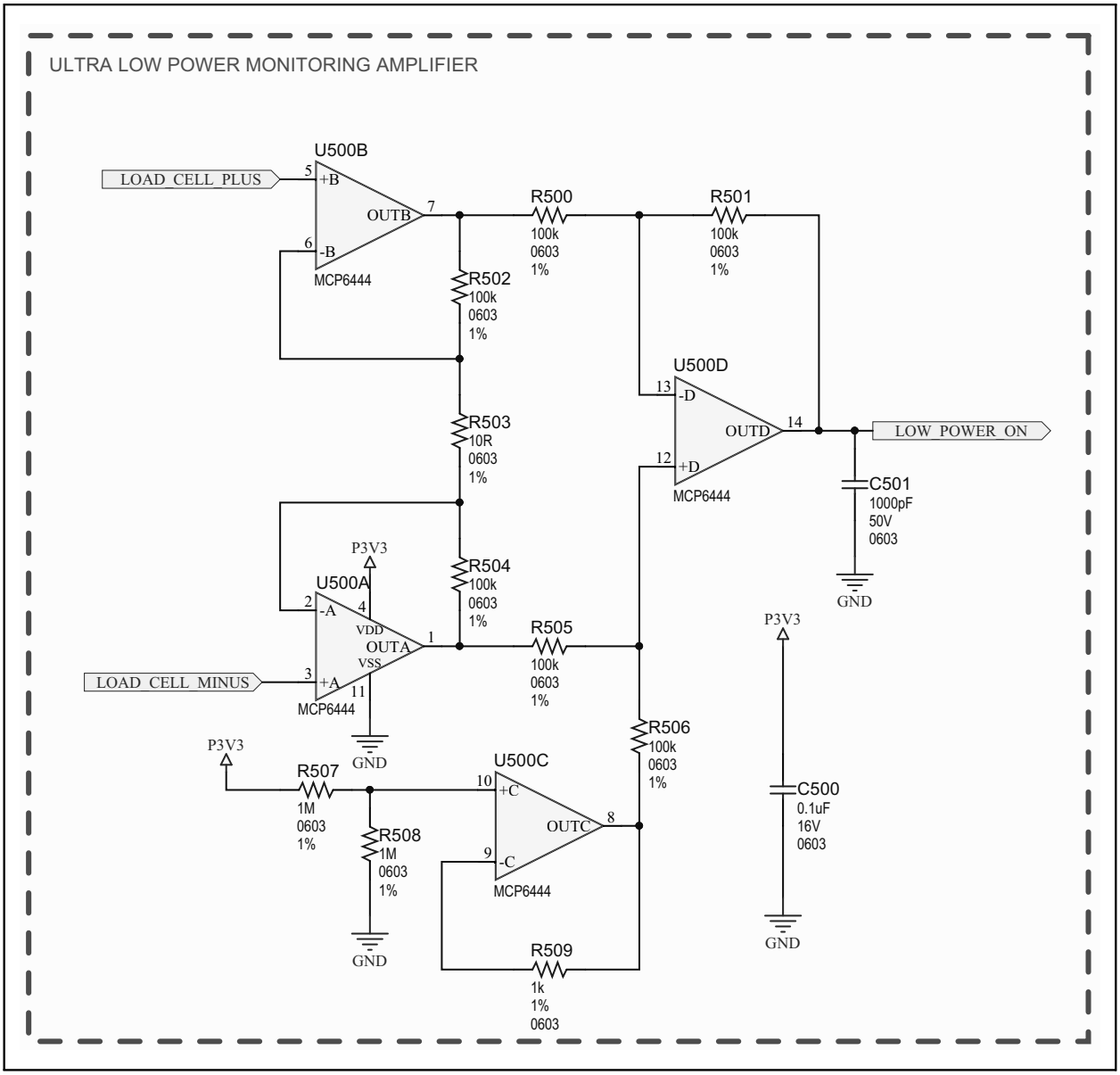

A.4 Weight Scale Board - Schematic 4

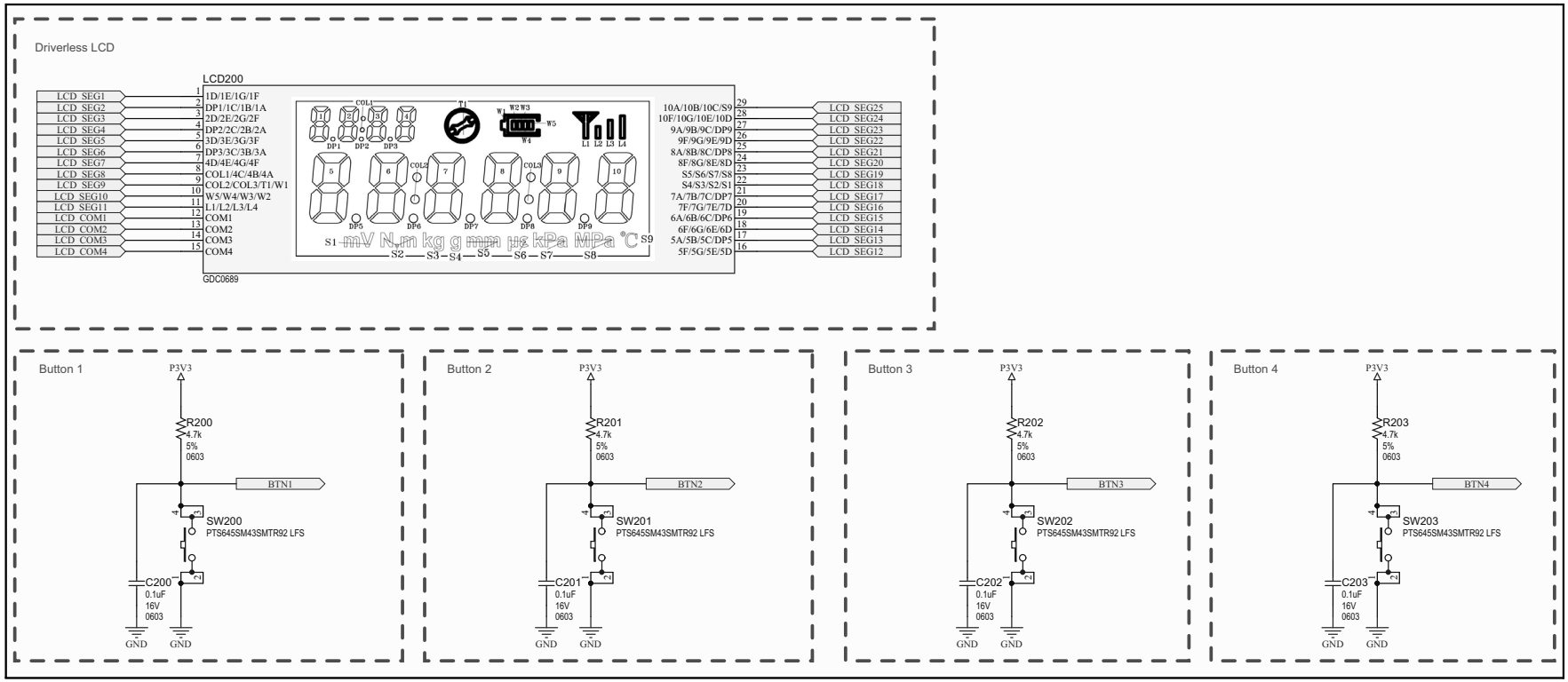

A.5 Weight Scale Board - Schematic 5

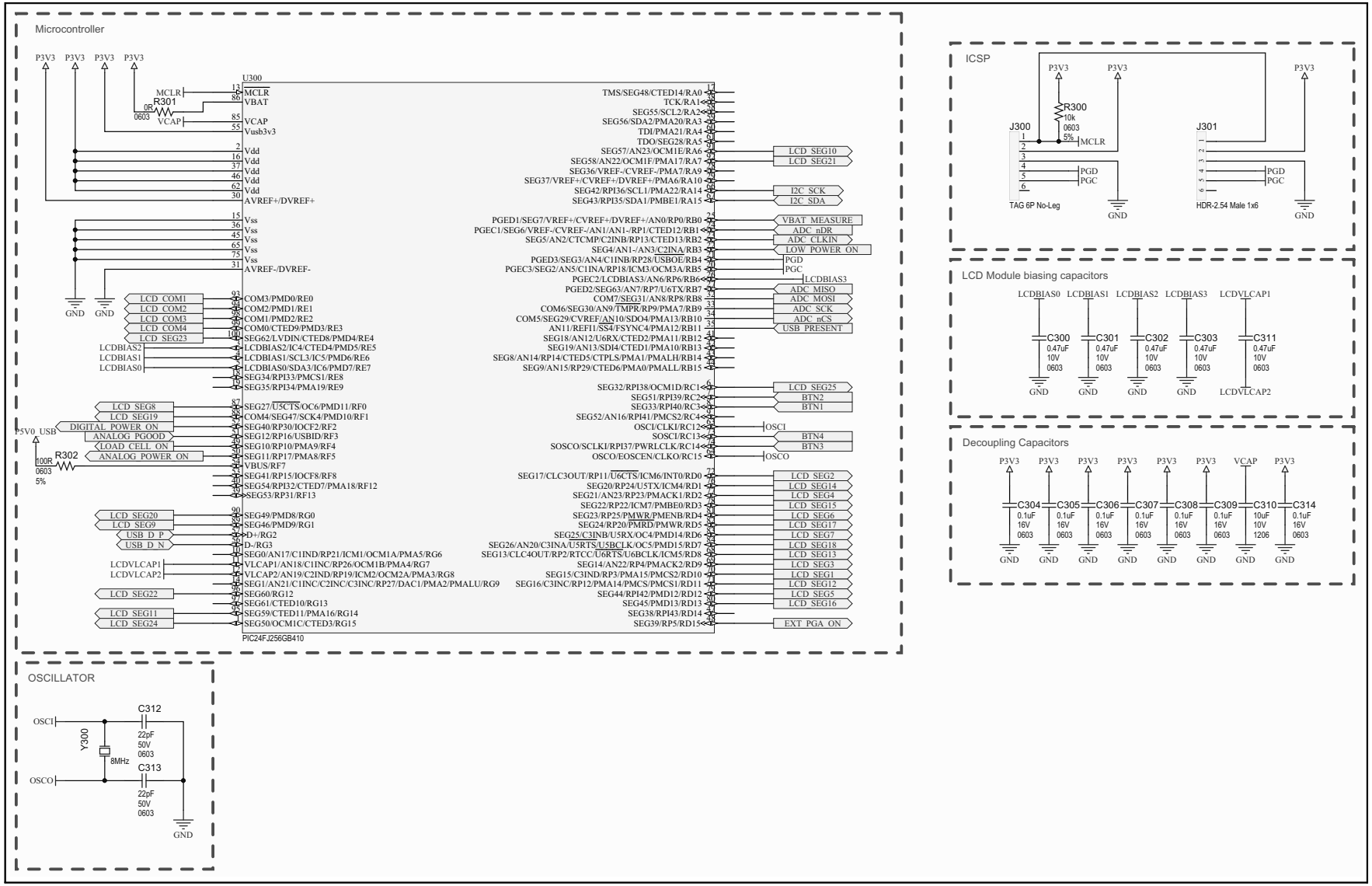

A.6 Weight Scale Board - Top Silk

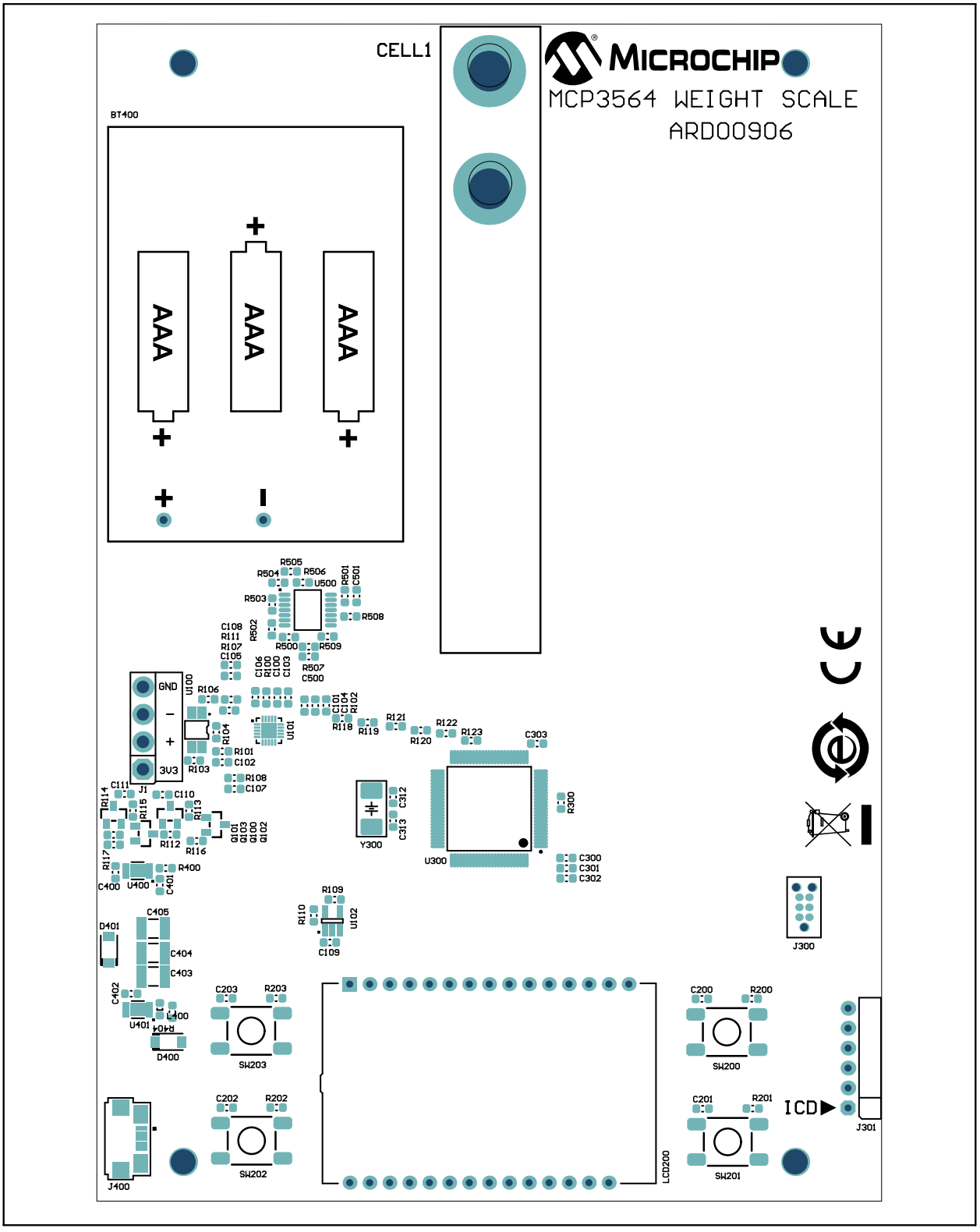

A.7 Weight Scale Board - Top Copper and Silk

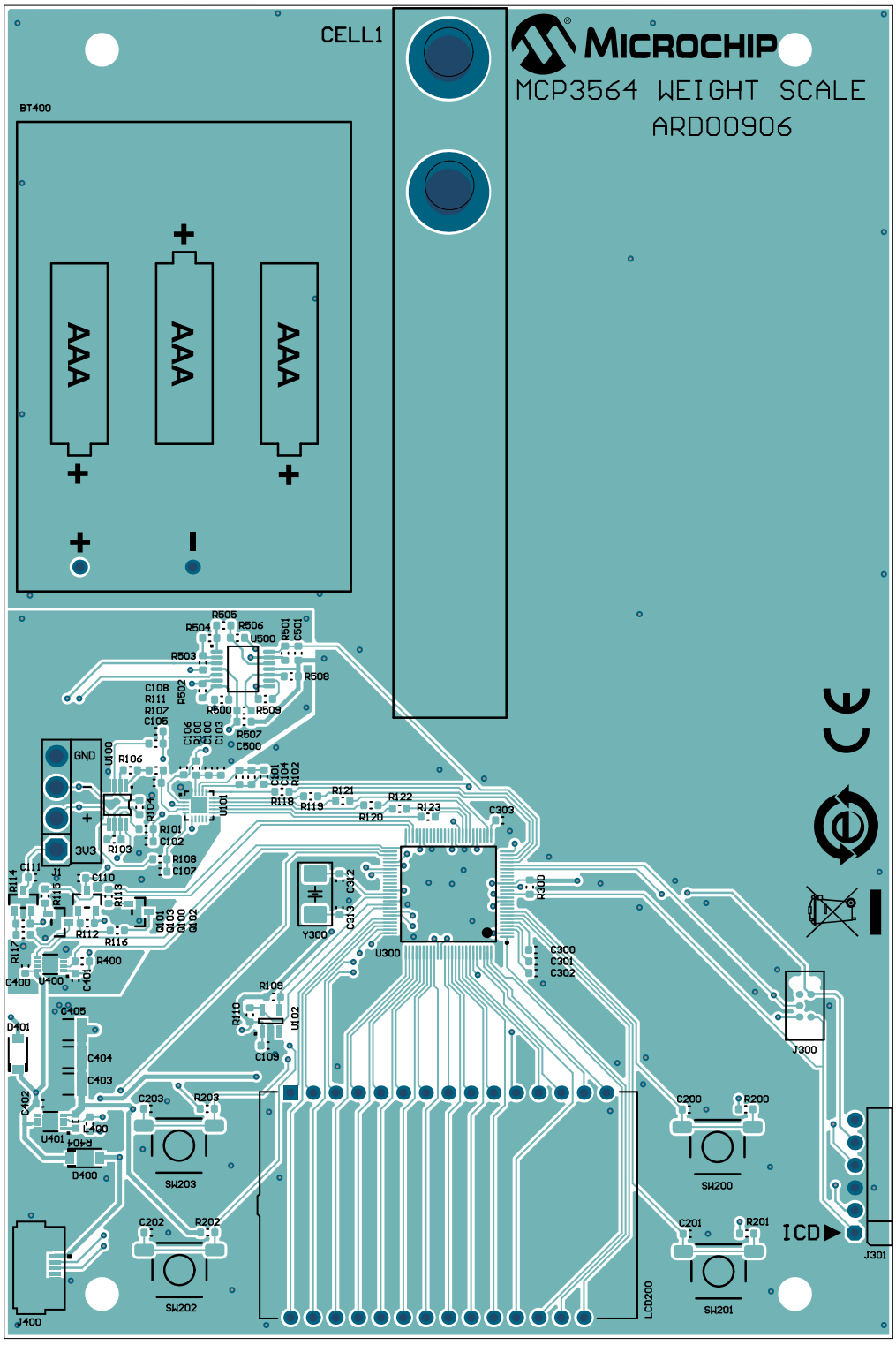

A.8 Weight Scale Board - Top Copper

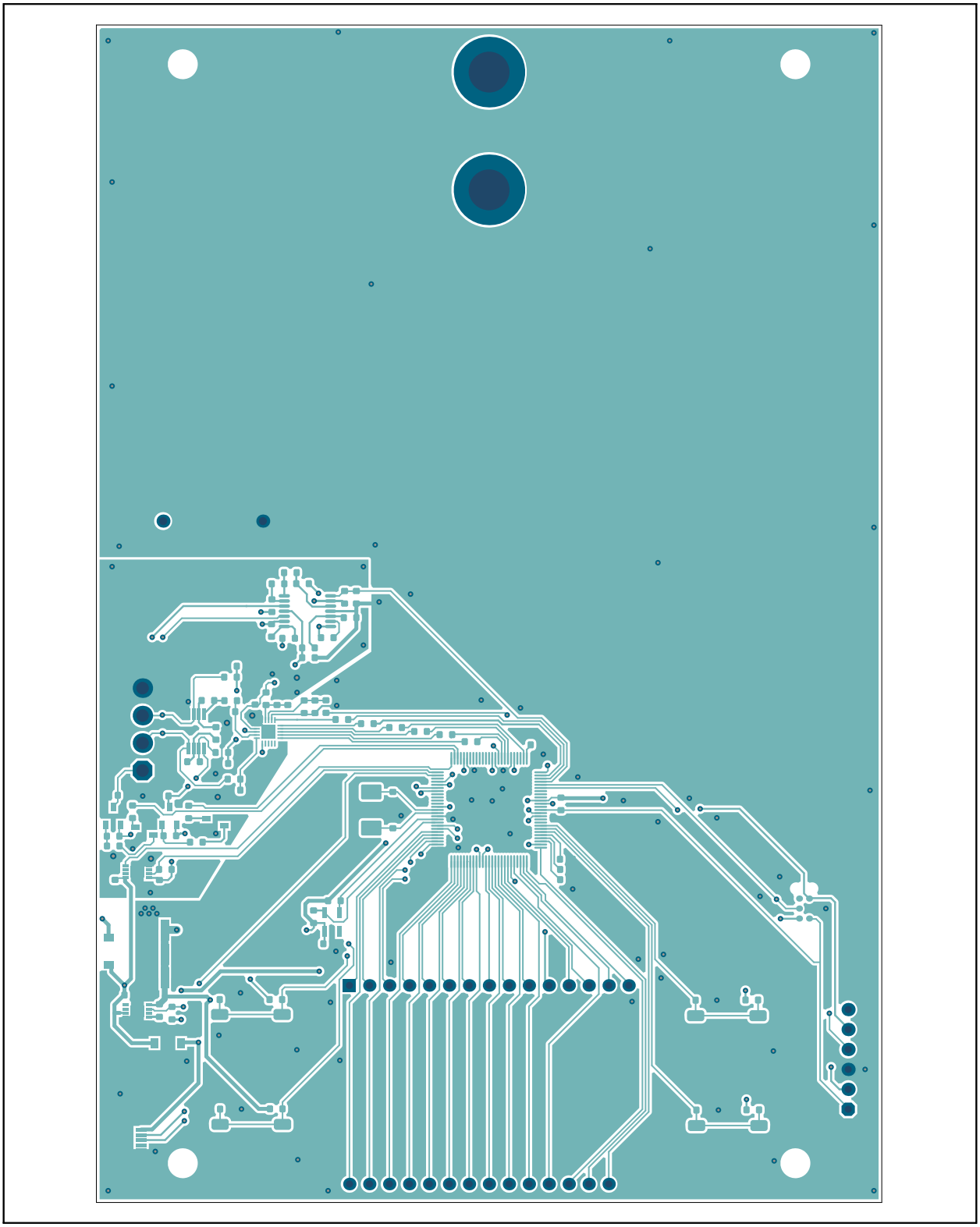

A.9 Weight Scale Board - Bottom Copper

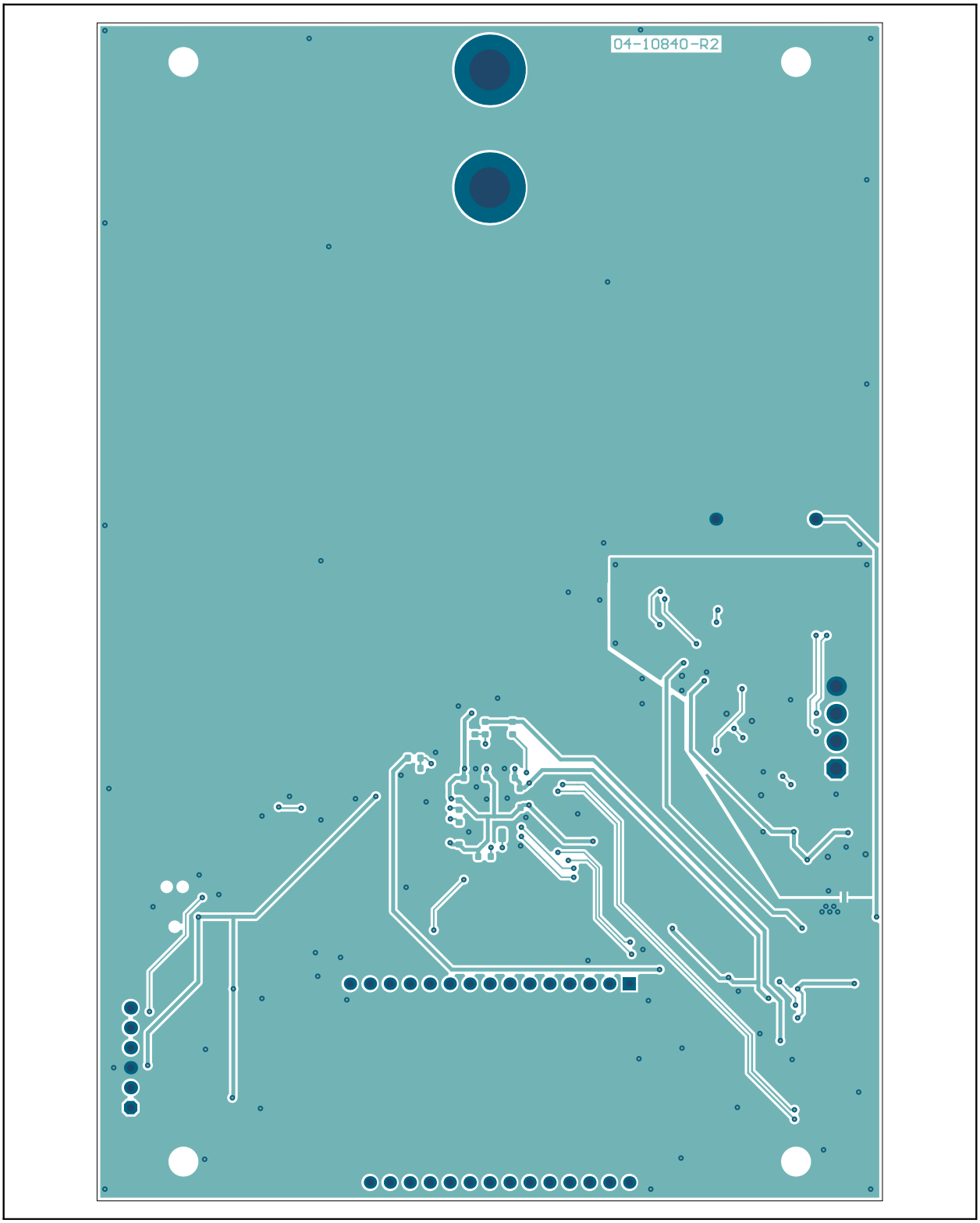

A.10 Weight Scale Board - Bottom Copper and Silk

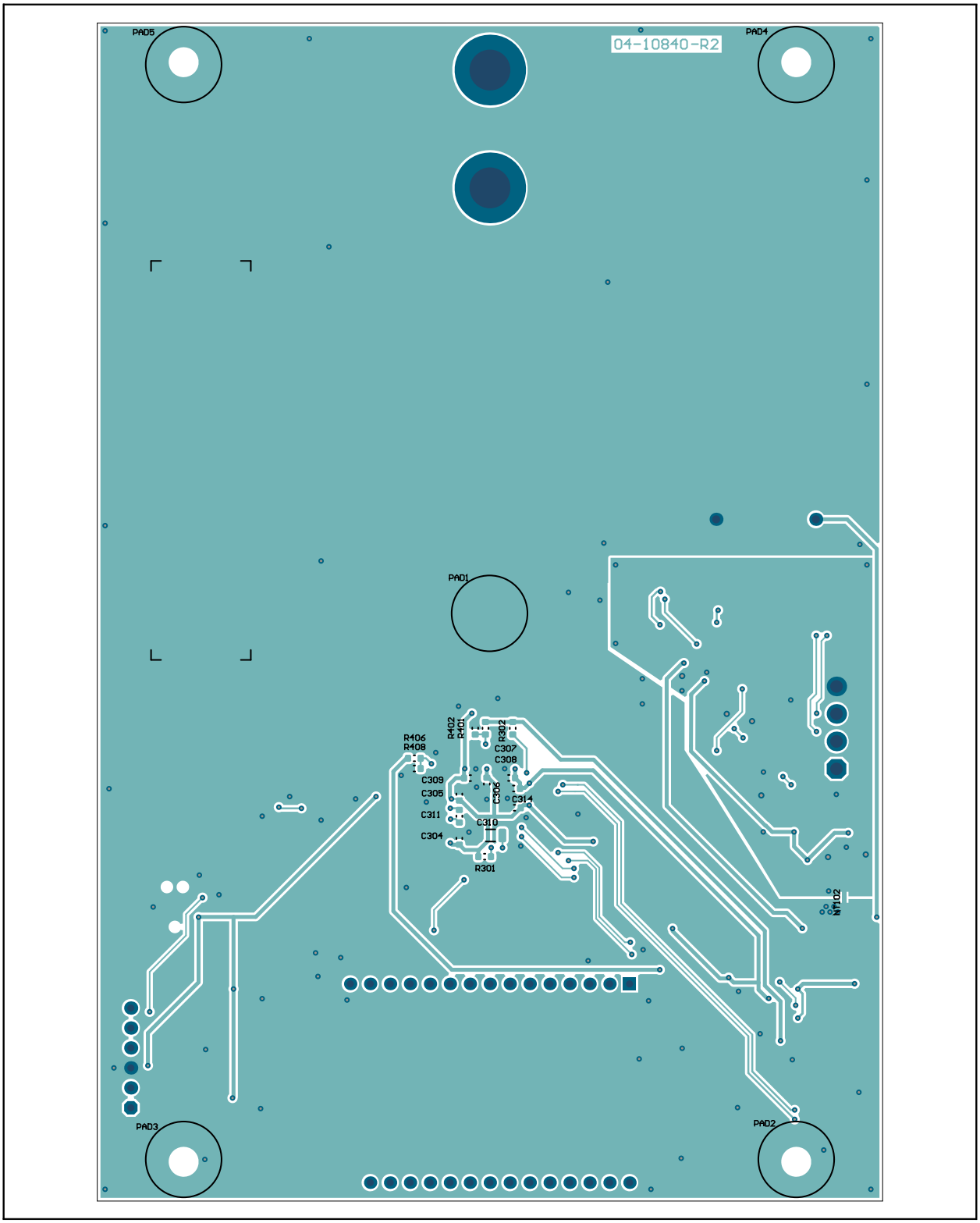

A.11 Weight Scale Board - Bottom Silk

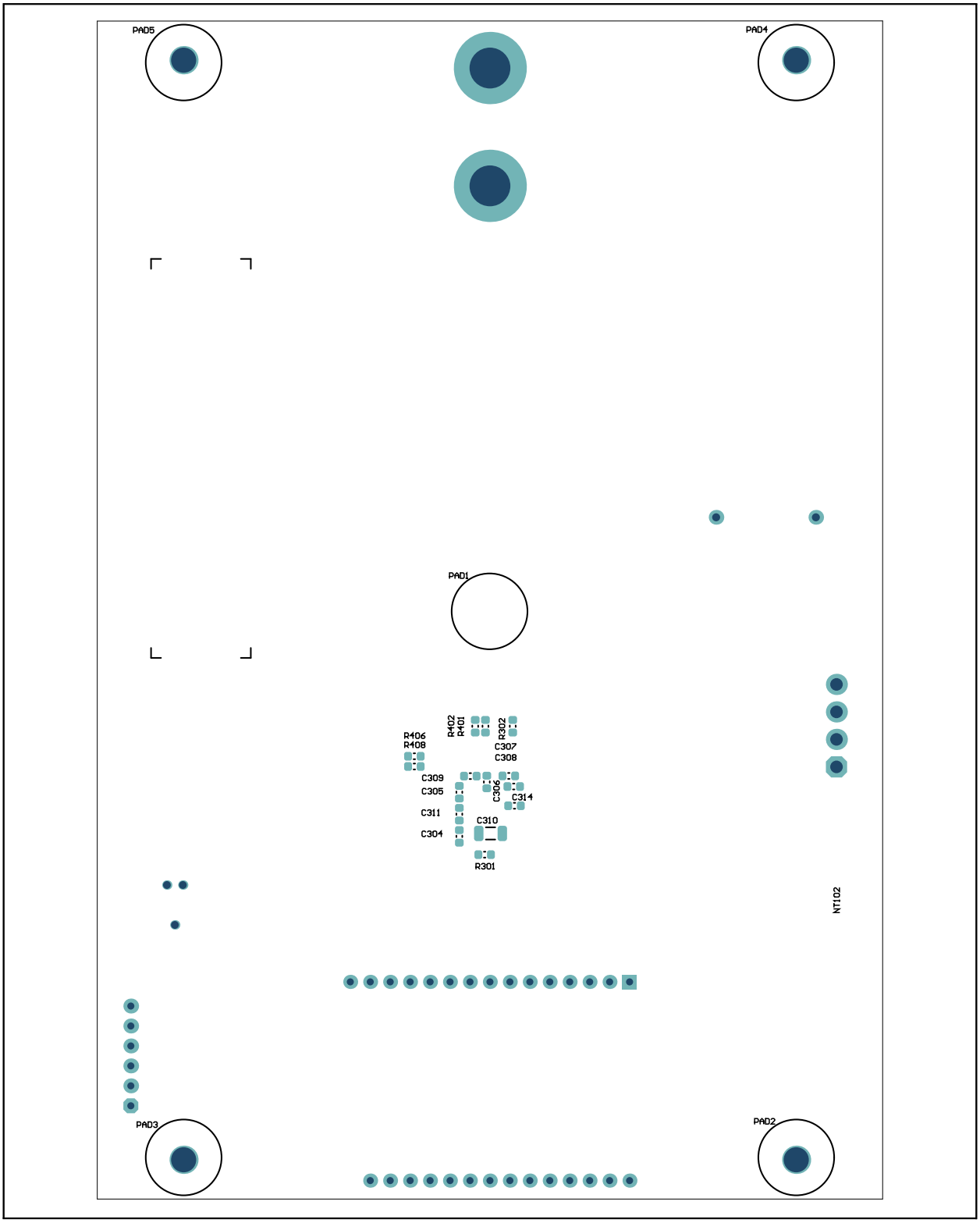

NOTES:

Note the following details of the code protection feature on Microchip devices:

- Microchip products meet the specification contained in their particular Microchip Data Sheet.
- Microchip believes that its family of products is one of the most secure families of its kind on the market today, when used in the intended manner and under normal conditions.
- There are dishonest and possibly illegal methods used to breach the code protection feature. All of these methods, to our knowledge, require using the Microchip products in a manner outside the operating specifications contained in Microchip's Data Sheets. Most likely, the person doing so is engaged in theft of intellectual property.
- Microchip is willing to work with the customer who is concerned about the integrity of their code.
- Neither Microchip nor any other semiconductor manufacturer can guarantee the security of their code. Code protection does not mean that we are guaranteeing the product as "unbreakable."

Code protection is constantly evolving. We at Microchip are committed to continuously improving the code protection features of our products. Attempts to break Microchip's code protection feature may be a violation of the Digital Millennium Copyright Act. If such acts allow unauthorized access to your software or other copyrighted work, you may have a right to sue for relief under that Act.

Trademarks

ISBN: 978-1-5224-5214-0

For information regarding Microchip's Quality Management Systems, please visit www.microchip.com/quality.

Worldwide Sales and Service

AMERICAS

Corporate Office
2355 West Chandler Blvd.
Chandler, AZ 85224-6199
Tel: 480-792-7200
Fax: 480-792-7277
Technical Support:
http://www.microchip.com/support
Web Address:
www.microchip.com

Atlanta
Duluth, GA
Tel: 678-957-9614
Fax: 678-957-1455

Austin, TX
Tel: 512-257-3370

Boston
Westborough, MA
Tel: 774-760-0087
Fax: 774-760-0088

Chicago
Itasca, IL
Tel: 630-285-0071
Fax: 630-285-0075

Dallas
Addison, TX
Tel: 972-818-7423
Fax: 972-818-2924

Detroit
Novi, MI
Tel: 248-848-4000

Houston, TX
Tel: 281-894-5983

Indianapolis
Noblesville, IN
Tel: 317-773-8323
Fax: 317-773-5453
Tel: 317-536-2380

Los Angeles
Mission Viejo, CA
Tel: 949-462-9523
Fax: 949-462-9608
Tel: 951-273-7800

Raleigh, NC
Tel: 919-844-7510

New York, NY
Tel: 631-435-6000

San Jose, CA
Tel: 408-735-9110
Tel: 408-436-4270

Canada - Toronto
Tel: 905-695-1980
Fax: 905-695-2078

ASIA/PACIFIC

Australia - Sydney
Tel: 61-2-9868-6733

China - Beijing
Tel: 86-10-8569-7000

China - Chengdu
Tel: 86-28-8665-5511

China - Chongqing
Tel: 86-23-8980-9588

China - Dongguan
Tel: 86-769-8702-9880

China - Guangzhou
Tel: 86-20-8755-8029

China - Hangzhou
Tel: 86-571-8792-8115

China - Hong Kong SAR
Tel: 852-2943-5100

China - Nanjing
Tel: 86-25-8473-2460

China - Qingdao
Tel: 86-532-8502-7355

China - Shanghai
Tel: 86-21-3326-8000

China - Shenyang
Tel: 86-24-2334-2829

China - Shenzhen
Tel: 86-755-8864-2200

China - Suzhou
Tel: 86-186-6233-1526

China - Wuhan
Tel: 86-27-5980-5300

China - Xian
Tel: 86-29-8833-7252

China - Xiamen
Tel: 86-592-2388138

China - Zhuhai
Tel: 86-756-3210040

ASIA/PACIFIC

India - Bangalore
Tel: 91-80-3090-4444

India - New Delhi
Tel: 91-11-4160-8631

India - Pune
Tel: 91-20-4121-0141

Japan - Osaka
Tel: 81-6-6152-7160

Japan - Tokyo
Tel: 81-3-6880- 3770

Korea - Daegu
Tel: 82-53-744-4301

Korea - Seoul
Tel: 82-2-554-7200

Malaysia - Kuala Lumpur
Tel: 60-3-7651-7906

Malaysia - Penang
Tel: 60-4-227-8870

Philippines - Manila
Tel: 63-2-634-9065

Singapore
Tel: 65-6334-8870

Taiwan - Hsin Chu
Tel: 886-3-577-8366

Taiwan - Kaohsiung
Tel: 886-7-213-7830

Taiwan - Taipei
Tel: 886-2-2508-8600

Thailand - Bangkok
Tel: 66-2-694-1351

Vietnam - Ho Chi Minh
Tel: 84-28-5448-2100

EUROPE

Austria - Wels
Tel: 43-7242-2244-39
Fax: 43-7242-2244-393

Denmark - Copenhagen
Tel: 45-4450-2828
Fax: 45-4485-2829

Finland - Espoo
Tel: 358-9-4520-820

France - Paris
Tel: 33-1-69-53-63-20
Fax: 33-1-69-30-90-79

Germany - Garching
Tel: 49-8931-9700

Germany - Haan
Tel: 49-2129-3766400

Germany - Heilbronn
Tel: 49-7131-72400

Germany - Karlsruhe
Tel: 49-721-625370

Germany - Munich
Tel: 49-89-627-144-0
Fax: 49-89-627-144-44

Germany - Rosenheim
Tel: 49-8031-354-560

Israel - Ra'anana
Tel: 972-9-744-7705

Italy - Milan
Tel: 39-0331-742611
Fax: 39-0331-466781

Italy - Padova
Tel: 39-049-7625286

Netherlands - Drunen
Tel: 31-416-690399
Fax: 31-416-690340

Norway - Trondheim
Tel: 47-7288-4388

Poland - Warsaw
Tel: 48-22-3325737

Romania - Bucharest
Tel: 40-21-407-87-50

Spain - Madrid
Tel: 34-91-708-08-90
Fax: 34-91-708-08-91

Sweden - Gothenberg
Tel: 46-31-704-60-40

Sweden - Stockholm
Tel: 46-8-5090-4654

UK - Wokingham
Tel: 44-118-921-5800
Fax: 44-118-921-5820